INFRA-RED SPECTRUM OF HAFNIUM

by

P. GONDHALEKAR, B.Sc., A.R.C.S.

Thesis presented to the University of London

for the degree of Doctor of Philosophy

MARCH 1970

ABSTRACT

The construction and operation of microwave excited hafnium discharge tubes is described. The electrodeless discharge, excited by microwaves at a frequency of 2450 MHz., provides a steady and intense emitter of the hafnium spectrum free of impurity lines. The wavenumbers of 521 infrared Hf I lines, falling within 1.0 - 2.5 μm have been measured to an average accuracy of 0.05 cm^{-1}. The relative intensities of these lines which lie outside the strong water vapour absorption regions, have been measured and corrected for the varying wavelength response of the detector.

Two hundred and twenty spectral lines have been assigned to the known energy levels of Hf I; the greatest difference between the observed and the calculated wavenumbers is 0.1 cm^{-1}. The intensities of the lines have been used to confirm the term assignments. A theoretical calculation (assuming intermediate couplings) of the positions of the levels of the even configurations $5d^4$, $5d^36s$ and $5d^26s^2$ of Hf I is presented. An empirical relation which gives a better fit with the observed levels of the configuration $5d^26s^2$ has been derived and new levels have been assigned to the configuration $5d^36s$.

CONTENTS

TABLES

ILLUSTRATIONS

CHAPTER I

INTRODUCTION

Hafnium was the last but one stable element to be discovered in the earth's crust; its discovery was announced by Coster and Van Hevesy in 1923[56]. Between 1923 and 1954, extensive analysis of the hafnium spectrum in the near UV and the visible regions was carried out to determine the Hf I energy level scheme. The Zeeman patterns of 200 lines were measured to classify the terms. Volume III of the Atomic Energy Levels[32] lists 109 even and 104 odd levels of Hf I; the total orbital angular momentum quantum number of all the levels and most of the Landè g-values have also been listed.

The analysis of the hafnium spectrum before 1954 was hampered by impurities in the hafnium samples used, the most serious impurity being zirconium. This early work was carried out by burning samples of hafnium, or hafnium oxide, in silver arcs operated in air. The hafnium spectrum was obscured over large spectral regions by strong and complex band systems of hafnium oxide. In 1958, Corliss and Meggers[16] reanalysed the hafnium spectrum in the wavelength range 1284.88-12043.08 Å using a hafnium sample of relatively high purity such that only the strongest impurity lines were observed. In this work a microwave excited electrodeless discharge in hafnium halide lamps was used and the overlapping oxide bands were absent.

In the research programme described in this thesis, the hafnium line list was extended to 2.5 μm; since the spectrum up to 1.0 μm had been analysed by previous workers[16], the present work was confined to wavelengths longer than 1.0 μm. Corliss et. al.[16] had investigated the spectrum in the wavelength region 1.0 - 1.2 μm using photographic methods. The sensitivity of photographic emulsions falls rapidly above 1.0 μm and, by using a cooled lead sulphide detector it was possible to detect some of the weak lines missed by the photographic methods. It was established,

by comparing the wavenumbers of the more intense lines observed by Corliss et. al.[16] with the present measurements, that the overall accuracies of the two sets of wavenumbers were comparable.

The infrared spectrum of hafnium was obtained using a one metre Czerny-Turner spectrometer and a cooled lead sulphide cell detector; the source was a microwave electrodeless discharge in a quartz tube containing hafnium iodide. The sample of hafnium sponge used to prepare the hafnium iodide contained 3% zirconium; use of such a sample could lead to serious difficulties in identifying the hafnium lines, but the difference between the sublimation temperatures of the hafnium and zirconium iodides was used to obtain pure hafnium iodide in the lamps. The detailed preparation of the lamps is described in Chapter 2. The intensities of most of the lines were measured (Chapter 3) and put on a uniform scale in order to aid the classification of the spectral lines[57,58].

The term designations have been made by previous workers[32] for only a few of the 109 even energy levels of Hf I. The term designation of levels can be very useful in comparing the observed intensities of the spectral lines with the calculated intensities and thus aid level classification of lines. The lowest even configurations of Hf I are probably the configurations $5d^26s^2$, $5d^36s$ and $5d^4$ and, since these configurations are probably not perturbed by other configurations, the positions of the levels of these configurations were calculated. These calculations, based on the assumption of intermediate coupling, are described in Chapter 4.

CHAPTER 2

EQUIPMENT

2.1. Introduction

An intense, stable and relatively long lived spectroscopic source can be obtained by microwave excitation of an electrodeless discharge in a tube containing the halide of an element. It was shown by Forrester et. al.[1] that for microwave excited mercury discharge the output optical power was high for input electric power. The microwave excited discharge was ideal for accurate measurement of wave-numbers as the spectral lines emitted by the discharge are quite narrow.

The method of construction of the sources has been evolved by a number of workers[2,3,4,5,6]. Tomkins et. al.[6] constructed a number of sources containing various elements in the form of halides; the sources were filled with an inert gas to initiate a discharge. These workers indicated a number of ways of excluding the impurities present in the samples of the elements, from the discharge tubes. The method of Tomkins et. al. formed the basis of the method used for preparing the hafnium sources and is described in Section 2.2.

A Czerny-Turner spectrometer was used to measure the wavenumbers of the hafnium lines. This spectrometer exhibits a large fraction of the theoretically possible resolution and was ideal for accurate measurement of wavenumbers of spectral lines. The basic optical system of a Czerny-Turner spectrograph was described as early as 1889. The optical arrangement of this spectrograph forms a perfect image as the light rays travel the same distance from the object (entrance slit) to the image. The corrective property of the optical system applies only to one line in the focal plane (the line which is the same distance as the entrance slit from the spectrograph axis) and the spectrograph forms sharp images only in a very

narrow spectral range. The optical system was, therefore, not suitable for photographic spectroscopy but was most attractive for use in a monochrometer. A systematic analysis of the optical arrangement was carried out by Fastie (1952)[8], who showed that the aberration corrective arrangement of the spherical mirrors left only astigmatism as a serious aberration. The effects of astigmatism and image curvature can be removed by use of matched curved slits. A Czerny-Turner spectrometer was modified for higher resolution and for use in the 1.0-2.5 μm region by replacing the original straight slits by a matched pair of curved slits and by employing an improved calibration system. The operation of the spectrometer to obtain the infrared spectrum of hafnium is described in Section 2.3.

In photographic spectroscopy the unknown spectrum and the calibration standards are recorded on the same photographic plate and the wavelengths of the spectral lines are determined by interpolation between the standards. The wavenumbers of the infrared lines can be measured by similar interpolation technique using the molecular emission and absorption bands and the overlapping orders of the inert gas spectra as standards. The method is of limited application in the 1.0-2.5 μm region because of lack of accurate and well distributed standards. In the infrared region, the spectral lines are recorded by scanning the spectrum across the exit slit by rotating the grating and the lines are recorded on a moving chart. The accuracy of the wavenumbers of the lines depends on the smoothness and precision of the mechanical drives which rotate the grating and move the chart. In order to minimise the dependence on the grating and the chart drives, it is necessary to have as many closely spaced standards as possible. The Edser-Butler fringes recorded simultaneously with the unknown spectrum provide an accurate, closely spaced wavenumber scale. The details of producing and recording the Edser-Butler fringes are given in Section 2.4. of this chapter.

2.2. Light Sources

The vacuum system used for preparing the hafnium lamps was as shown in the block diagram of Fig. 2.1. The mercury diffusion pump was capable of pumping the vacuum system down to a pressure of 1.0×10^{-6} torr. The part of the vacuum system where the lamps were prepared (Fig. 2.2., the trap Tp was connected at point P shown in Fig. 2.1.) was isolated from the diffusion pump by liquid nitrogen cooled traps. This was to prevent mercury from diffusing into the tube and contaminating the discharge. The silica tube shown in Fig. 2.2., was cleaned by boiling concentrated nitric acid in the tube; the nitrogen dioxide liberated from the hot nitric acid had a powerful cleansing effect on silica. The tube was washed about ten times with distilled water to remove all the acid. The tube was degassed by heating it to about 1000°C by a furnace, while it was maintained under high vacuum. A R.F. discharge in neon was started in the silica tube after it had been degassed for about an hour and the neon spectrum was monitored by a direct vision spectrometer. The neon gas was pumped out after 15 mins. if impurity bands were observed in the discharge. A fresh batch of gas was introduced in the tube and discharged and the spectrum was monitored; this process was repeated till no impurity bands were observed.

Hafnium iodide was used in the sources prepared during the present project as the sources filled with the iodide of an element were more stable and long-lasting than sources filled with other halides[6]. The hafnium iodide was prepared in the glass capsule C (Fig. 2.2.). The capsule was cleaned with hot nitric acid, dried and filled with 50 mg. of hafnium and 150 mg. of iodine and was pumped down to about 1.0×10^{-5} torr and sealed. The mixture of hafnium and iodine was baked for about an hour at 400°C to produce the iodide of hafnium and of the impurities present in

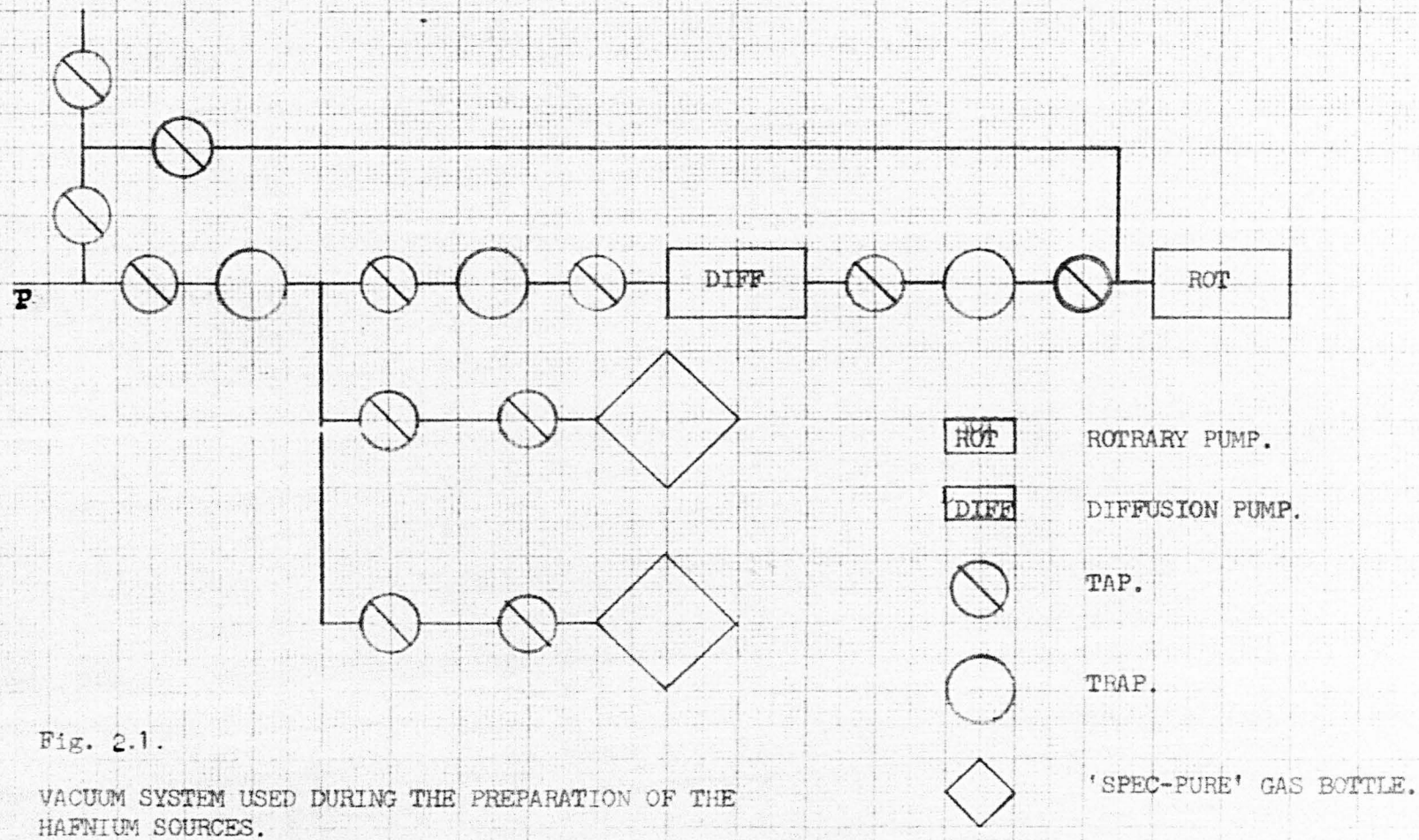

Fig. 2.1.

VACUUM SYSTEM USED DURING THE PREPARATION OF THE HAFNIUM SOURCES.

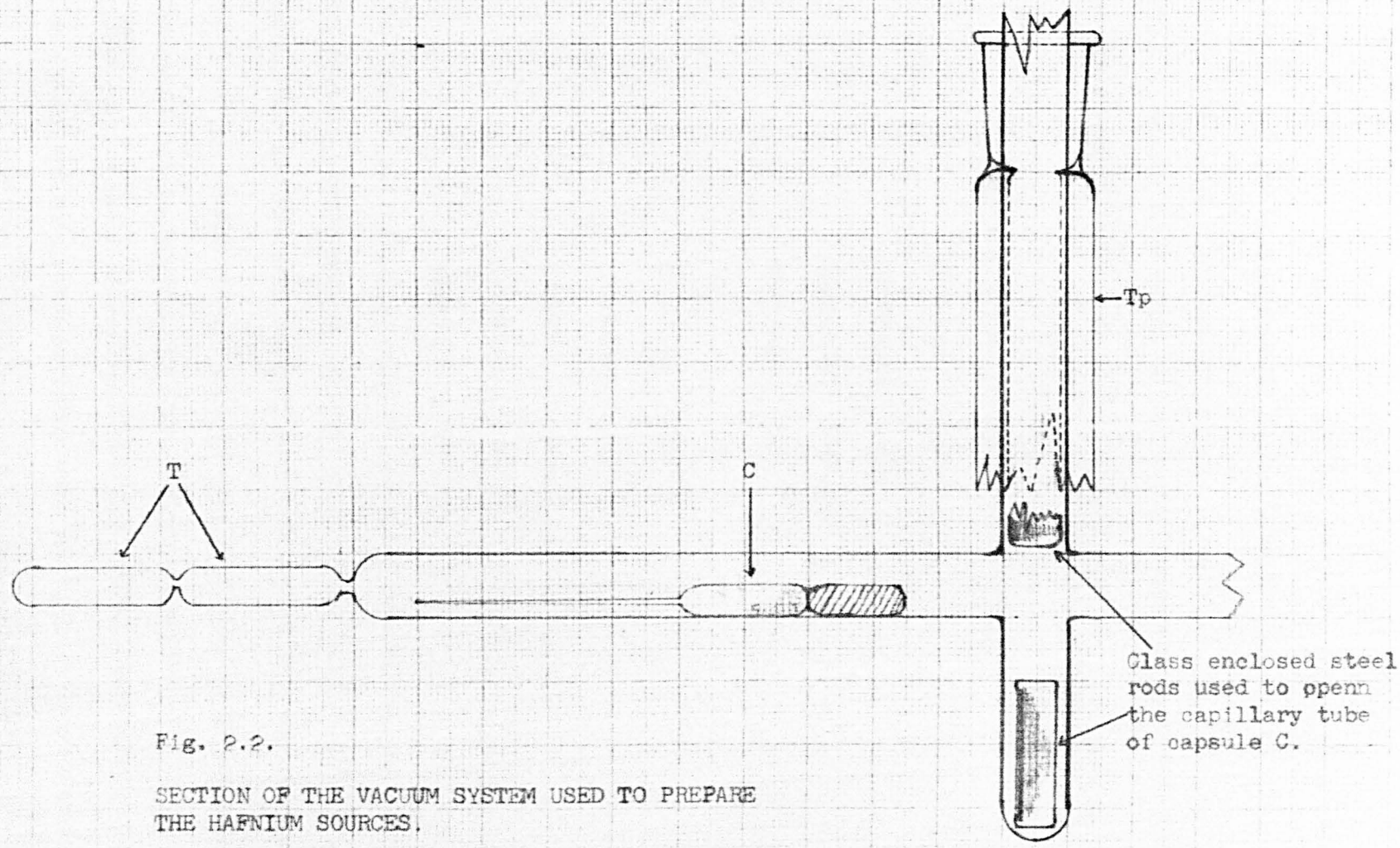

Fig. 2.2.

SECTION OF THE VACUUM SYSTEM USED TO PREPARE THE HAFNIUM SOURCES.

sample of hafnium. The spectroscopic analysis of the hafnium sponge, acquired from Koch-Light Laboratories Ltd., is given in Table 2.1. (only impurities with more than 10 ppm. concentration have been listed). Zirconium, magnesium, tantalum and ~~silicon~~ nickel were the most serious impurities and precautions had to be taken to ensure that the iodides of these elements were kept out of the tube T (Fig. 2.2.). The sublimation temperatures of hafnium iodide and the iodides of the major impurities in the hafnium sponge are given in Table 2.2.

TABLE 2.1.

The major impurities in the hafnium sponge

Hafnium	99.8%
Zirconium	3.0%
Magnesium	540 ppm.
Niobium	100 "
Iron	90 "
Tantalum	200 "
Aluminium	45 "
Copper	40 "
Silicon	40 "
Nickel	100 "

The end of the capillary tube of capsule C was opened under vacuum and the capsule was warmed by a bunsen burner till hafnium iodide just sublimed. The iodides with melting points below 400°C., the excess iodine and some hafnium iodide were pumped out as the capsule C was warmed. These iodides condensed in the trap Tp (Fig. 2.2.). The capsule C was then moved up to the tubes T and a thin film of hafnium iodide (just enough for the tube to appear coloured) was sublimed into the tubes. The capsule C was warmed till it was just possible to sublime the hafnium iodide in order to

TABLE 2.2.

Melting and sublimation temperatures of some iodides

Hafnium iodide	under vacuum, sublimes at 400°C
Ferric iodide	melts and decomposes
Cuprous iodide	melts at 605°C
Zirconium iodide	decomposes at 600°C
Magnesium iodide	decomposes at 700°C
Nickel iodide	melts at about 250°C
Niobium iodide	" " " "
Tantalum iodide	" " " "
Aluminium iodide	" " " "
Silicon iodide	" " " "

exclude from the tubes T the iodides with melting points higher than 400°C. A R.F. discharge in 'spec-pure' argon or neon was started in tubes T and monitored with a direct vision spectrometer. The discharge was maintained till the hafnium spectrum was just visible; the gas was then pumped out to remove the iodine produced by the decomposition of hafnium iodide. A fresh batch of 'spec-pure' gas at a pressure of about 2 torr was introduced in the tubes and the tubes were sealed off. A number of hafnium sources, two at a time (5 mm bore and 10 cm. long), containing argon, neon or no filler gas at all were made and operated successfully.

The discharge in the sources filled with argon or neon was started by a tesla coil. The sources without any filler gas had to be warmed, to build up iodine vapour pressure, before a discharge could be initiated. The operation of the sources to obtain the infrared spectrum of hafnium is described in the next chapter.

The sources were operated successfully for several periods of about 10 hours. The argon filled sources failed after about seventy hours of operation. This may have been due to the drop in the pressure inside the tube due to the absorption of argon by hot silica[14]. The spectrum in the visible and near ultra-violet, of the light emitted by the hafnium sources was photographed using a Hilger medium quartz spectrograph. There was no difference between the spectra emitted by the neon and the argon filled sources, but the spectrum emitted by the sources without any filler gas was slightly brighter. With a Hartmann diaphragm, the iron spectrum was photographed on either side of the hafnium spectrum and the hafnium lines were identified with an accuracy of $\pm$ 1 Å, using iron lines as standards. None of the lines could be ascribed to the major impurities present in the hafnium sponge, nor could any lines be identified as mercury lines.

2.3. Dispersive System

The spectrometer used to obtain the infrared spectrum of hafnium was a one metre, f/6 plane grating spectrometer in a Czerny-Turner mounting. The 15 x 12 cms., 600 lines per mm., Bausch and Lomb grating was mounted on a lead-screw driven turn-table with which the spectrum could be scanned across the exit slit. The grating (No. 35-53-17-57) was blazed for 2.5 μm in the first order and the grating orders could be selected by manually rotating the turn-table through large angles relative to the lever arm. The spectrometer was originally rather sensitive to vibrations as the detector unit and the optics were mounted on separate bases. In order to minimise the effects of vibrations the two units were set up on a single firm base and were housed in light-tight boxes to eliminate stray light.

The optics of the Czerny-Turner spectrometer has been discussed by Fastie[7,8] and it has been shown[17] that by using a straight entrance slit

the image at the exit slit is parabolic. The length of the entrance slit which can be used to obtain the theoretically possible resolution is given by[8],

$$L = 10\lambda(F/W)^3 \qquad 2.1.$$

and the wavelength error from the centre to the end of the exit slit is

$$\Delta\lambda = \lambda/8(F/L)^2 \qquad 2.2.$$

where L is the length of the slits

λ is the wavelength of the radiation

F is the focal length of the collimating mirror

W is the distance between the entrance and the exit slits.

For radiation of 2 μm, straight slits no longer than 0.16 cms could be used to obtain the theoretically possible resolution. With a straight exit slit 2 cms long there could have been a wavenumber error of 0.04 cm^{-1} between radiation emerging from the centre and the end of the exit slit. The astigmatism and the wavenumber difference between the radiation emerging from the centre and the end of the exit slit can be corrected by using a pair of matched, curved entrance and exit slits. For the 15 cms wide grating, Hilger and Watt curved slits, 2 cms long and radius of curvature of 11.25 cms (4.5 ins.) were used. The slits were placed so that the light beams passing to the collimating mirrors were not obstructed by the grating.

The infrared radiation in the 1.0-2.5 μm range was detected with a cooled lead sulphide cell. The Kodak "Ektron" lead sulphide cell (Type N2) was 1 x 5 mms in size and was mounted on a quartz base. The cell was mounted on the end of a 1 in. diameter copper rod, Fig. 2.3., and cooled by dipping the rod in a mixture of solid carbon dioxide and acetone stored in a dewar flask. To maintain the low temperature of the cell the dewar flask was refilled with solid carbon dioxide once every hour. The surface of the cell was kept free of condensed water vapour by enclosing

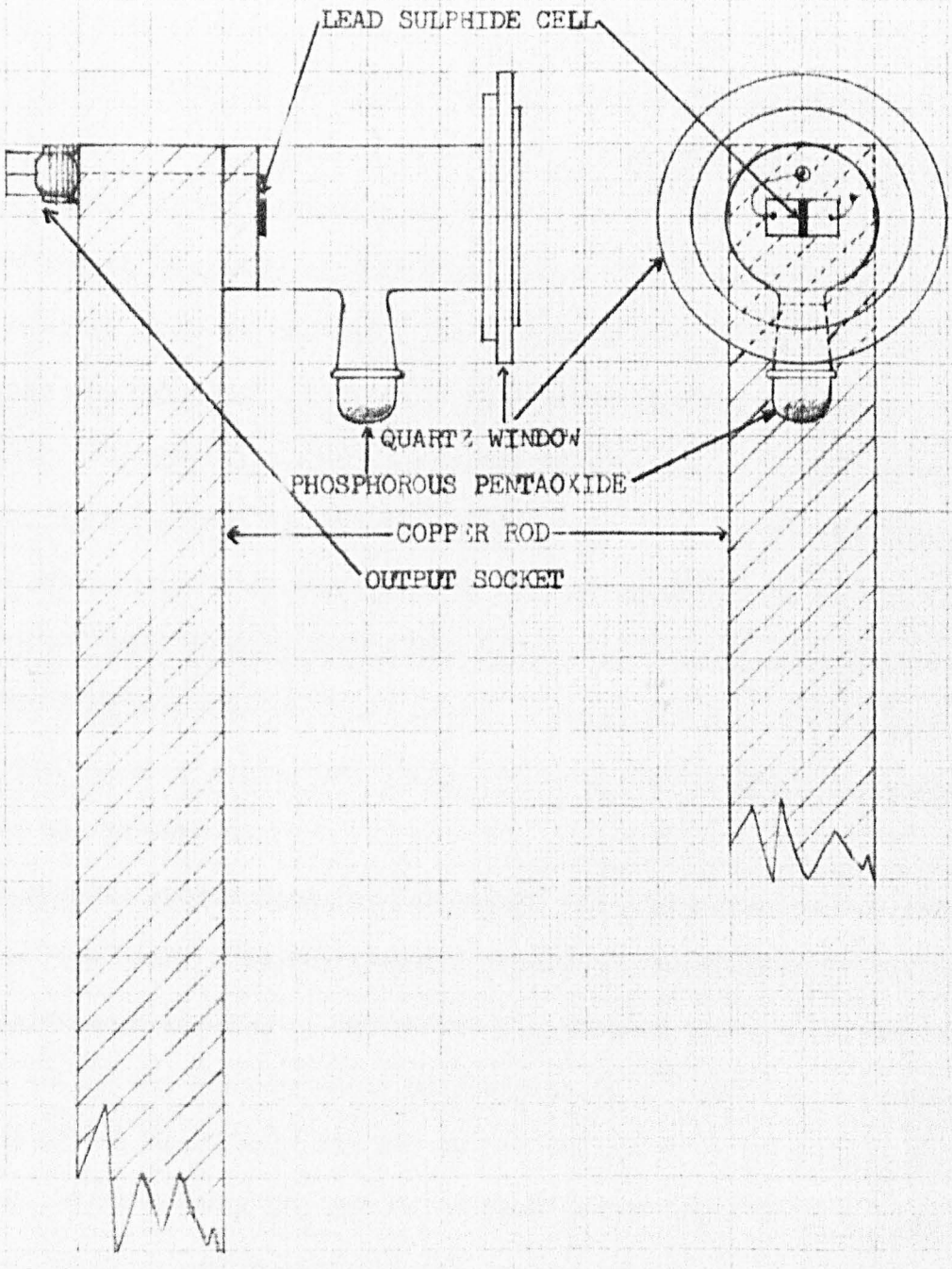

Fig. 2.2.

COOLING SYSTEM FOR THE LEAD SULPHIDE CELL

the cell in a glass tube, the air inside the tube was dessicated with phosphorous pentaoxide. The end of the glass tube was closed by a quarts window which was kept slightly above room temperature by a heater wound along its circumference.

The output from the lead sulphide cell was of the order of 1 μV. This signal had to be amplified to drive a pen recorder and amplification of at least 100 db.was necessary to record most of the weak lines. A Barr and Stroud frequency selective amplifier with a maximum gain of about 120 db centred at 20 Hz was used. To obtain an alternating signal the light beam was 'chopped' at 20 s^{-1} by a sectored disc rotated at 10 s^{-1}. The signal to noise ratio could be increased by using a phase sensitive amplifier (manufactured by Brookdeal Electronics Ltd.), but the time constant of the amplifier was too high for the amplifier to be useful at the scanning speed used to record the hafnium spectrum. In the present system, the limiting time-constant (about 1 sec.) was that of the pen recorder and for the scanning speed used (0.35 Å / sec.) almost 99% of the signal amplitude was developed.

The optical system used for 'chopping' the light beam was as shown in Fig. 2.4. The light from the spectral source SS was focused by the mirror CM_1 on to the chopper blade CB. The mirror CM_2 focused the beam on to the entrance slit. The chopper motor revolved at 10 s^{-1} and the alternate quadrants of the blade were cut out to let the spectral beam pass onto the mirror CM_2. The mirrors CM_1 and CM_2 reflected the light beam in opposite directions as this arrangement reduced coma[7], giving a better image at the entrance slit.

The vertical tilt of the slits was adjusted by visually observing the strong neon lines (between 5000 Å and 6500 Å) as they were scanned across the exit slit. The lines were scanned in both directions and the slit mountings were rotated in the plane of the

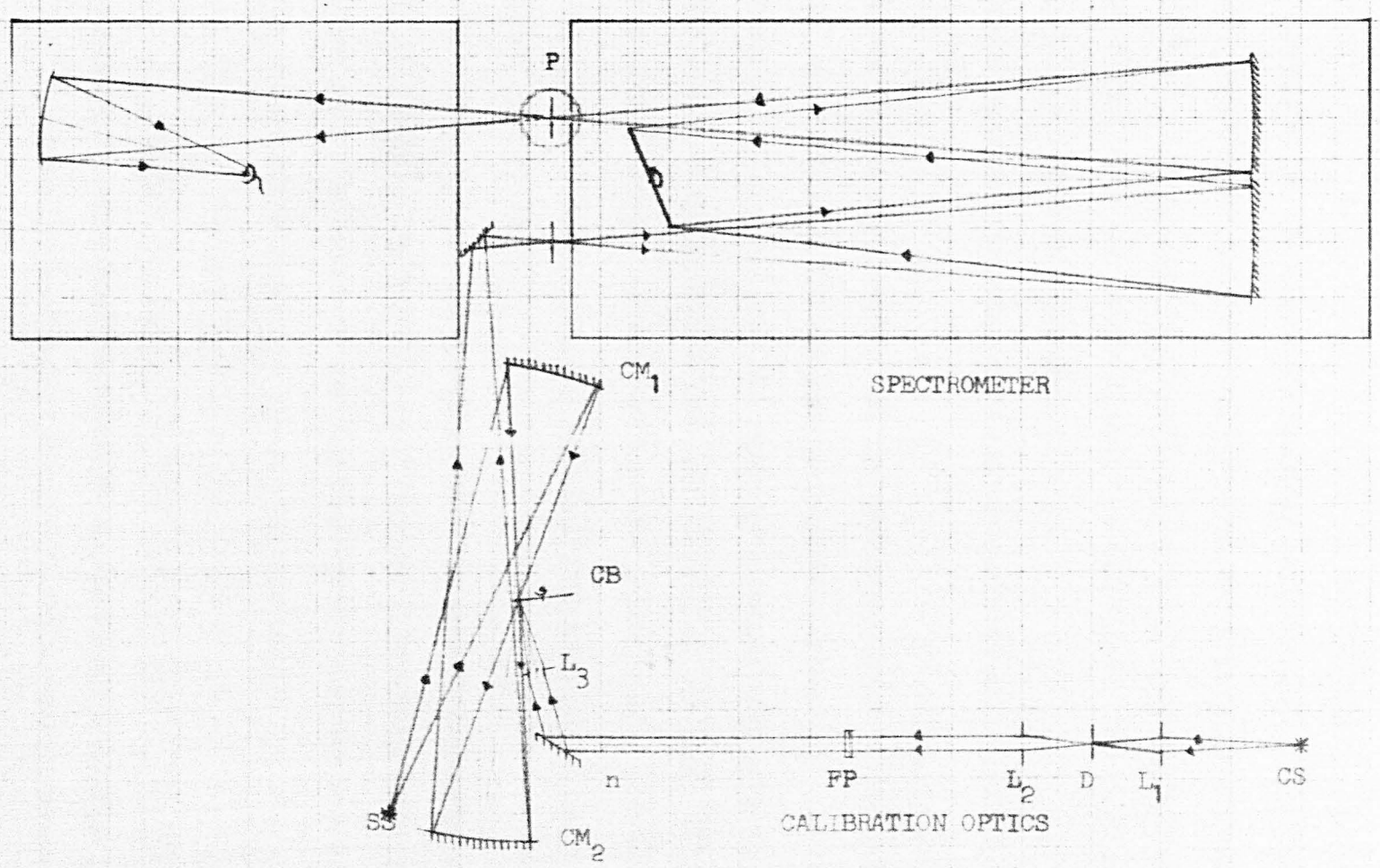

Fig. 2.4.

SPECTROMETER THE ENTRANCE AND THE EXIT SLIT OPTICS.

slits till the images, at the exit slit, matched the slit. The 'tilt adjustment' was repeated for lines observed in four grating orders and with slits narrow enough for the lines to be just visible. In all the cases the images of the lines were matched with the slit. The neon lines were then detected by the lead sulphide cell and the slits were rotated perpendicular to the plane of the slits (the axis of rotation coincided with the slits) till the output signal was maximised. The vertical tilt of the slits was then readjusted.

The calibration spectrum or the fringes are generally recorded by (10, 41, 42),

1) Illuminating a small portion of the entrance slit with the calibrating beam and reflecting the emergent beam onto a detector.
2) Illuminating, alternately, the whole of entrance slit with the calibrating or the spectral beam and separating the beams at the exit slit. The alternate illumination of the entrance slit and the separation of the beams at the exit slit can be achieved by two choppers rotated synchronously.

In the first method the two beams have to be well separated at the entrance slit to prevent the overlap of images at the exit slit. The overlap can shift the peaks of the spectral lines which can result in large errors in the wavenumbers of the lines. In this method, the detectable radiation flux is decreased because of the short length of the slit available for the spectral beam. The main disadvantage of the second method is the decrease in the signal to noise ratio caused by the stray radiation in front of the detector cell being chopped at the same frequency as the spectral beam. The two methods also require two detectors and two amplifiers for the spectral and the calibration signals respectively. The second method has the advantage of allowing the use of the entire length of the slits for both the beams. This method can be modified by replacing

the chopper at the exit slit by a "AND gate system" to separate the amplified outputs due to the two beams. The two beams can then be detected by a single cell and the signals amplified by a single amplifier.

A system of "AND" gates, using six diode gates[30,31] (Fig. 2.5.) was built to separate sections of a waveform by synchronous switching of the gates. The operation of the gates can be seen from Fig. 2.6. where the waveform A represents a 20 Hz square wave used to test the gates. A small 10 Hz signal was input to the Schmidt trigger, the two outputs from the Schmidt trigger were amplified (Fig. 2.6. B and C) and were used to trigger the gates. The gates were able to separate alternate "top-hats" of the waveform A to produce the waveform D and E. The two outputs were rectified and smoothed and input to the two-pen recorder. The gate outputs were linear up to 2 V peak-to-peak input. This was the order of output signal voltage expected due to the two beams and the gate system was well suited for separating a waveform produced by the two light beams.

The gate system was tested by detecting the spectral and the calibration beams. To obtain a signal due to the calibration beam the "calibration optics" shown in Fig. 2.4. were set up. Front aluminised mirrors were mounted on the uncut quadrants of the chopper blade CB, which reflected the calibrating beam from source CS onto the concave mirror CM_2, which focused the beam on the entrance slit. When the blade CB was rotated, the spectral and the calibration beams were alternately focused onto the entrance slit. The trigger pulse for the Schmidt trigger was obtained from a phototransistor mounted opposite the point where the chopper blade intercepted the spectral beam. The phototransistor was illuminated by a small lamp, light from which was chopped by the blade CB. For test purposes the Fabry-Perot interferometer FP (Fig. 2.4.) was removed and a strong signal from the source CS was detected by the lead sulphide cell. A λ6402 Å neon line was

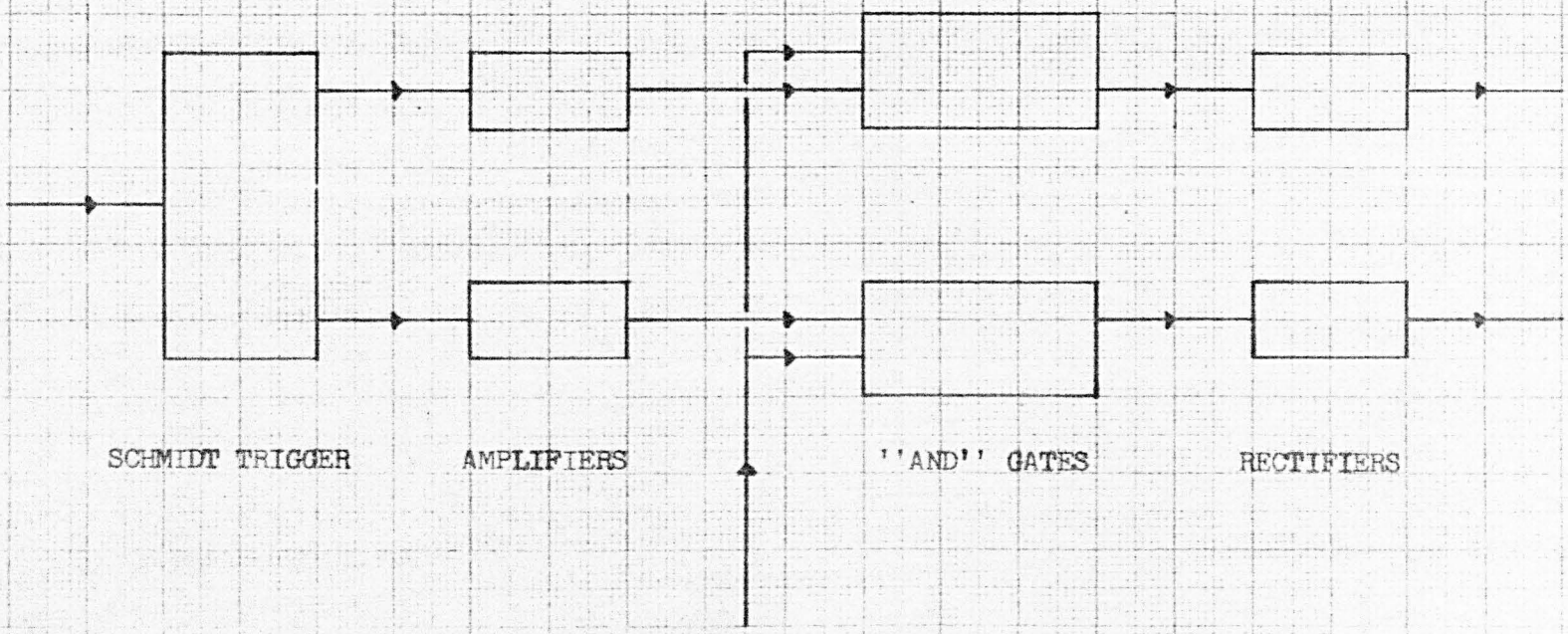

Fig. 2.5.

''AND'' GATE SYSTEM

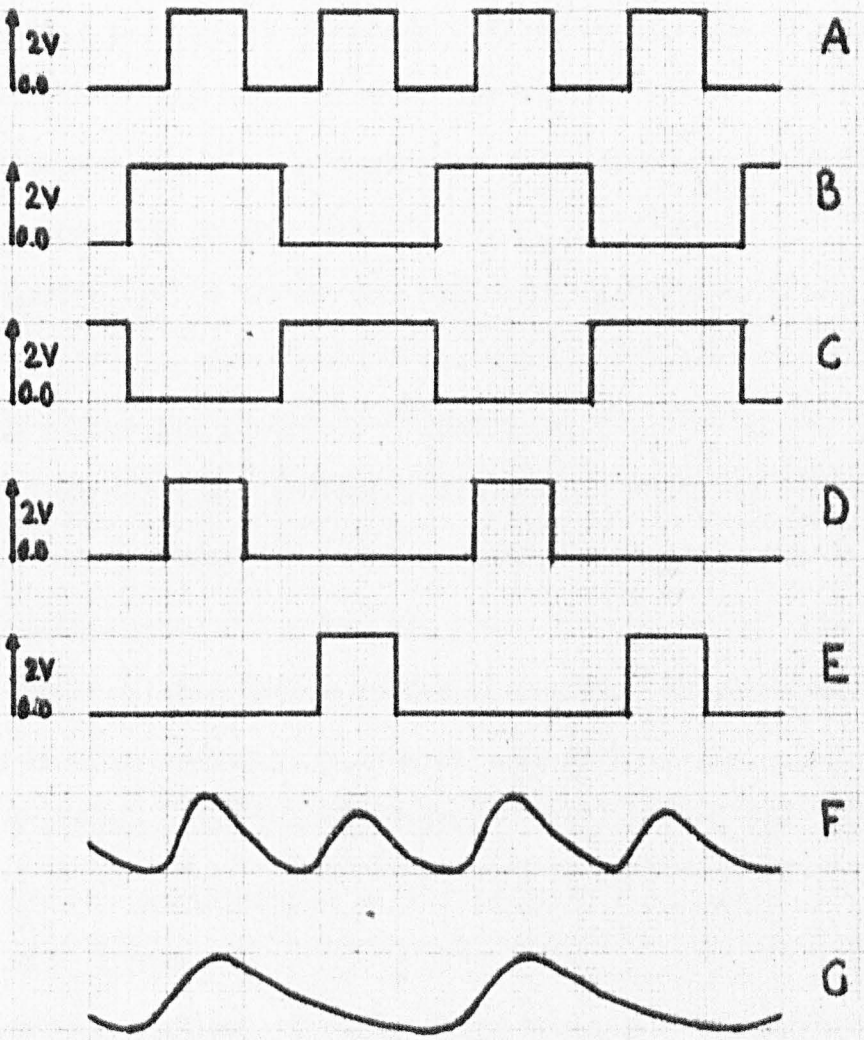

Fig. 2.6.

WAVEFORMS OF THE SIGNALS USED

TO TEST THE "AND" GATES.

also detected by the same lead sulphide cell and the combined signal was amplified by a wide-band amplifier (manufactured by Brookdeal Electronics Ltd.). The waveform of the amplified signal was as shown in Fig. 2.6.F. There was appreciable overlap of signals in the two output channels and the overlap increased when one of the signals was absent. The signal waveform in such a case was as shown in Fig. 2.6.G; in this case the overlapping signal was of the same order as the signal expected due to the beam and the overlapping signals could not be eliminated by reducing the width of the triggering pulse. The overlap of the signals on the two channels was primarily due to the low frequency distortion of the input signal. The electronic separation of the signals was abandoned as an amplifier with a good low frequency response was not immediately available.

To obtain the calibration fringes, the lower quarter of the entrance slit was illuminated by the calibrating beam, leaving the rest of the length of the slit for normal use. The beams were separated just enough to prevent the overlap of the images at the exit slit. To avoid delay in recording the hafnium spectrum, no changes were made in the optics. The production and detection of the Edser-Butler fringes used for calibrating the spectral records is described in the next section.

2.4. Calibration System

The interference method of calibrating spectrometers provides an accurate method for measuring the wavenumbers of spectral lines in the regions of spectrum where no suitable standards are available. This is particularly true of the infrared region (1.0-2.5 μm) in which the number of interferometrically measured standards are very few. The spectrum and the interference fringes were recorded simultaneously and the number of fringes per record was quite large (about one fringe per cm of chart). The method does not rely on the long term stability of the spectrometer.

The optical system used for interference calibration of the spectrometer was as shown in Fig. 2.4. Continuous radiation from the quarts iodide tungsten lamp CS was focused on the pin-hole diaphragm D by the lens L_1. The collimating lens L_2 directed a parallel beam of light on to the Febry-Perot etalon FP. The radiation emerging from the etalon was focused on the chopper blade CB by lens L_3. The front aluminised quadrants mounted on the chopper blade reflected the beam onto the concave mirror CM_2 which focused it on the lower quadrater of the entrance slit. The radiation emerging from the upper quarter of the exit slit was reflected onto the end of a flexible light guide which conducted the light to the photomultipler P. In order to record the Edser-Butler fringes, the photomultiplier was connected to a pen-recorder via a cathode follower.

The etalon can be considered to be an interference filter having maximum transparency for radiation satisfying the wavelength relation

$$N_e\lambda = 2dn\cos\phi \qquad 2.3.$$

where N_e is the etalon interference order

λ is the wavelength of the radiation

d is the etalon spacing

n is the refractive index of the medium between the plates

ϕ is the angle between the collimated beam direction and the etalon normal.

This relation can be expressed in terms of the wavenumber σ of the radiation transmitted with maximum intensity by

$$\sigma = AN_e \qquad 2.4.$$

where

$$A = (2dn\cos\phi)^{-1}$$

To register fringes of suitable character, the fiducial constant A had to be matched to the dispersing and resolving power of the spectrometer and an

etalon spacer 1 mm thick was necessary. Three steel ball-bearings, 1/16 ins. diameter, held in a thin aluminium annular disc formed a suitable spacer. With the etalon in axial position for maximum light intensity, a typical value of A was 3.1644 ± 0.0005 cm^{-1}. A 10 cms focal length lens was necessary as a collimator before the etalon. A good quality quartz lens was used, as this lens determined the fringe definition.

The interference fringes provided a set of fiducial marks whose separation corresponded to a constant wavenumber difference expressed by the constant A. Equation 2.4. can be regarded to be a dispersion relation giving the wavenumber of any spectral line whose position could be referred to the scale of the fringes. The wavenumber σ_1, of a spectral line of order N_1 can be expressed as

$$\frac{\sigma_1}{N_1} = \frac{\sigma_s}{N_s} + \left(\frac{A}{N_c}\right)(m + e_1 + e_2) \qquad 2.5.$$

where σ_s is the accurately known wavenumber of a neon standard

N_s is the order of the standard line

A is the fiducial constant

e_1 and e_2 are the additional fractions of a fringe.

m is the integer number of fringes between lines σ_1 and σ_s

N_c is the grating order of the band of continuous radiation used to produce fringes.

Two standard lines were recorded, one at each end of a record, the wavenumber of the standards were substituted for σ_1 and σ_s in the Eq. 2.5. to calculate A.

In Eq. 2.5., the unknown wavenumbers were expressed in terms of a constant, A. This constant was a function of the refractive index of the medium between the etalon plates, air in the present case. The refractive index of air can vary with temperature and pressure. This change over an

extended run can introduce serious errors in the wavenumbers of the lines. To reduce the effect of the temperature and the pressure change of the air to a negligible proportion, the etalon was housed in an evacuated chamber. A second factor controlling the value of the constant A was the expansion and the contraction of the etalon spacer. The heat conduction from the base of the vacuum chamber to the etalon and the spacer was reduced by mounting the etalon on brass rods tapered to a point. The spectrometer and the associated calibration system used to measure the wavenumbers of the hafnium lines emitted in the 1.0-2.5 um region was as shown in the photograph of Fig. 2.7.

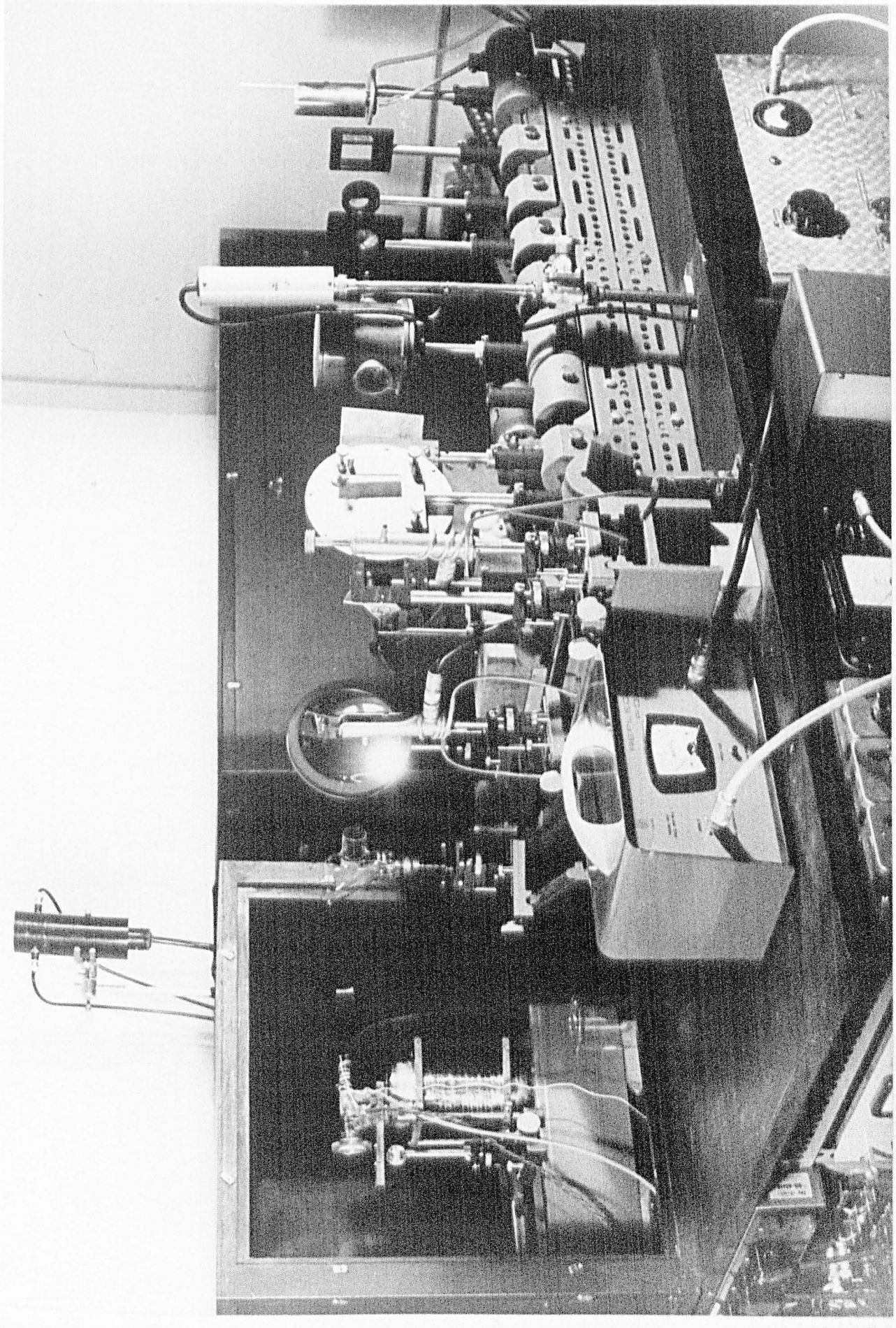

Fig. 2.7.

CHAPTER 3

EXPERIMENTAL PROCEDURE

3.1. Operation of Sources

The discharge in the hafnium iodide filled sources was excited by microwaves at a frequency of 2450 MHz. The microwaves were generated continuously by a Mullard JP2-02 magnetron which could be operated at a maximum power of 200 watts. A D.C. potential difference of about 1 kV had to be maintained across the magnetron. This potential difference was constant at about 1 kV for any current (in mA) drawn by the magnetron and provided a rough indication of the microwave power (in watts) output. The microwaves were passed by a coaxial cable to a tuneable cavity exciter[20], via a reflected power meter manufactured by Electromedical Supplies (EMS). The cavity (designed by Dr. E. B. M. Steers of Northern Polytechnic, London and supplied by EMS) was of silver plated brass and one inch in diameter. The cavity and the coaxial connector on the cavity was water cooled by circulating water through $\frac{1}{8}$ in. brass tube soldered round the cavity and the socket. The water cooling was necessary to prevent damage to the cavity and to the insulation of the socket when the sources were operated at high power.

The intensity of the discharge and the tuning of the cavity varied with the position of the sources in the cavity. The optimum tuning i.e. minimum reflected power, was possible when the tubes were held along the axis of the cavity. In order to ensure the axial position of the sources, the channel in the upper tuning stub of the cavity was machined to a diameter of 6 mms. The portion of the sources (O.D. 5 mms) projecting inside the tuning stub aligned the sources with the axis. The sources rested on a glass rod inside the cavity.

To obtain the hafnium spectrum, a hafnium iodide filled source was placed inside the cavity and the magnetron current was increased to 100 mA.

The discharge was started by a high frequency leak tester and the magnetron current was increased to its final value, usually 190 mA or 175 mA. The tuning stubs were adjusted to minimise the reflected power (usually of the order of 10 watts). The sources were allowed to warm-up for about 15 mins. before the spectra were recorded. During the first 10 mins. of the warm-up period the discharge was unstable and confined to the axis of the source. During this time the intensity of the hafnium lines increased while the intensity of the iodine lines and the bands decreased. After the first fifteen minutes no iodine bands were observed and only the strongest iodine lines (λ5119 Å and λ6337 Å) were seen; the discharge was stable and filled the source. The magnetron power and the reflected power stayed constant throughout a run, usually lasting for about six hours. After six hours of continuous operation, the intensity of the spectral lines increased by about 1% but there was no noticeable change in the width of the lines.

The microwave excited lamps emit predominantly the first spectrum and the strongest lines of the second spectrum. Several authors[6,21] have shown that the relative intensities of the lines of the first and the second spectrum vary with the vapour pressure of the element in the lamp. At low vapour pressure the lines of the second spectrum are relatively favoured whereas at high vapour pressure the first spectrum is enhanced. The vapour pressure in the lamps could be altered by changing the microwave power input to the cavity. During the analysis of the hafnium spectrum two records were obtained with magnetron current of 190 mA, and one record was obtained with magnetron current of 175 mA. It was not possible to record spectra at lower magnetron currents (e.g. 150 mA) as the spectra were too weak. The intensities of all lines recorded with the magnetron current of 175 mA had dropped by a factor of two-thirds compared to intensities of lines recorded with the magnetron current of 190 mA., no relative enhancement of any spectral lines could be observed. This seemed to indicate

a total absence of emission of Hf II lines in the 1.0 - 2.5 μm range, this was confirmed when attempts were made to fit the lines in the final line list to the known energy levels of Hf II; only one line could be assigned to the levels of Hf II, the accuracy of the fit was about 0.05 cm^{-1} and the assignment was probably coincidental. The details of classification of the spectral lines are given in Chapter 4.

3.2. Measurement of Wavenumbers

The slit widths necessary to detect all the lines emitted by the hafnium lamps would have decreased the resolving power of the spectrometer by a large factor and it would not have been possible to resolve either the hafnium spectrum or the calibration fringes. Slits wide enough to detect the majority of spectral lines without a large decrease in the resolving power of the spectrometer were selected as follows. With an entrance slit of 30 μm and an exit slit of 14 μm only the strongest hafnium lines were detected and the calibration fringes were very weak. The width of the entrance slit was increased to 50 μm and sections of hafnium spectrum were recorded with increasing exit slit width. With an exit slit of 30 μm almost 90% of the lines emitted by the hafnium lamps could be detected and the calibration fringes were of reasonable intensity throughout the 1.0 - 2.5 μm range. These slit widths were used for all the spectra recorded with the calibration fringes.

Wavenumbers of hafnium lines were measured using the first order of the 600 lines/mm grating of the spectrometer. Two settings of the grating, relative to the lever arm, were necessary to cover the whole of spectral range investigated during the present project. One grating setting covered the1.7 - 2.5 μm region and a second setting covered the 1.0 - 1.8 μm region. The blazed side of the grating was used for the 1.7 - 2.5 μm range but the reversed side was used for the 1.0 - 1.8 μm region as in this wavelength region the intensity of the light reflected from the reversed side was

higher than the intensity of light reflected from the blazed side. A Grubb-Parsons silicon infrared filter was used to eliminate the higher overlapping grating orders. This filter was also used when the spectrum in the 1.8 - 2.5 μm region was recorded and the second order 1.0 - 1.25 μm spectrum was recorded on the same chart. The two grating orders were sorted out by recording this region of the spectrum using a germanium filter in place of the silicon filter. The wavelength and the transmission characteristics of the two infrared filters were as given in Table 3.1.

TABLE 3.1.

Wavelength and Transmission Characteristics of the Infrared Filters

FILTER	CUT-OFF WAVELENGTH	TRANSMISSION
Silicon	1.0 μm	90 - 95%
Germanium	~ 1.5 μm	90 - 95%

A series of survey spectra (spectra recorded without calibration fringes) were obtained beforehand to identify spectral lines which were strong enough to overload the pen recorder. During the final analysis of the hafnium spectrum the output from the amplifier was attenuated to record the peaks of these strong spectral lines.

Selected neon lines (in the 0.58 - 1.0 μm region[24,25] and observed in higher grating orders) whose wavenumbers were known to an accuracy of 0.001 cm^{-1} were used to calibrate the fringes. The standards were recorded during a run by introducing at appropriate times an additional mirror to reflect the light from a neon source on to the entrance slit. The neon spectral source was a microwave excited neon discharge. Two standards, one at each end of the run, were essential and were used to calculate the fiducial constant A (Eq. 2.5). Additional neon standards were recorded in the regions of the spectrum where no hafnium lines were observed but where higher order neon lines were possible. The "gaps" in

the hafnium spectrum were selected from the survey runs and the neon lines were used to check the accuracy of the wavenumbers of the hafnium lines.

The positions of the hafnium lines relative to the calibration fringes were measured on a viewing box which had a metre rule which could be clamped parallel to the edge of the chart. A vertical line scribed on a transparent perspex setsquare was aligned with the peaks of the lines or the fringes and their relative positions were measured with a vernier scale scribed on the setsquare. The number of calibration fringes between the first neon standard and the hafnium lines, the grating order of the lines and the positions of the lines relative to the adjacent fringes were punched on a paper tape and the air wavenumbers of the lines were computed using Eq. 2.3. It was not necessary to know the grating order of the "band" of continuous radiation used to obtain the calibration fringes as the two neon standards recorded at the beginning and the end, respectively, of each run were used to calculate the fiducial constant A. In the regions of strong water vapour absorption (1.3 - 1.4 μm and 1.8 - 1.95 μm), hafnium lines coincident with the strong absorption lines could not be recorded. The absorption lines close to the hafnium lines shifted the positions of maximum intensity of the hafnium lines, reducing the accuracy of the wavenumbers of these lines. The details of the accuracy of the wavenumbers of the hafnium lines is given later in this section.

A spectral record consisted of a section of hafnium spectrum recorded by one pen of a two pen recorder and a section of calibration fringe trace recorded by the second pen. The "spectral beam" and the "calibration beam" had different path lengths and the time constants of the two detecting systems were also different; a correction was necessary for the "dynamic separation" of the two pens. The dynamic pen separation was necessary as the separation of the two pens held under tension, was different for a moving chart and for a stationary chart. The pen separation was obtained (18)

by recording "artificial lines" produced by detecting λ 6000 Å neon line on both the spectrum and the fringe recording systems. The image of the neon lamp covered the whole of the entrance slit and the grating was moved manually till the neon line was detected at the exit slit. The exit slit was opened to 50 μm and the output from the two detecting systems was monitored. Both signals were then cut-off by intercepting the neon light beam at the entrance slit. The light beam was allowed to pass for the time required to register a spectrum line (about 5 secs) and the separation (in cms.) between the two artificial lines was the required correction. The dynamic pen separation was independent of the strength and the duration of the signal and was treated as a constant.

The slit widths used for recording spectral charts with calibration fringes were too small to detect the weak lines emitted by the hafnium lamps. The width of the entrance slit was increased to 175 μm to record these weak lines. The purity of the spectrum deteriorated because of the wide entrance slit and it was impossible to obtain the calibration fringes. The wavenumbers of the weak lines were measured by linear interpolation between two adjacent strong lines. The strong lines as near the weak lines as possible were used and only lines free of perturbing adjacent lines were measured. The wavenumbers of the strong lines were obtained from the charts recorded with calibration fringes. The accuracy of the weak lines was less than the accuracy of the lines measured from charts with calibration fringes.

The accuracy of the wavenumbers of the hafnium lines was determined by the following factors,

I The irregularity in the grating drive

II The irregularity in the chart drive

III The human error in measuring the positions of the lines relative to the fringes

IV The different time-constants of the two detecting systems.

V The dissimilar illumination of the grating face by the light from the neon and the hafnium sources. This would result in a difference in shape of the neon and the hafnium spectral lines.

VI The different effect of the temperature and the pressure change on the neon standards and the hafnium lines recorded in different orders.

The errors due to (I) and (II) were reduced by using calibration fringes for measuring the wavenumbers of the spectral lines. The irregularities in the grating or the chart drive were neglected unless these occurred between the fringes used for measuring the positions of the lines relative to the fringes. Such irregularities were noted and the accuracy of the line in question was reduced. The details of the accuracy code are given later in this section. The errors due to (III) were reduced by measuring each line at least twice; if the two wavenumbers differed by more than 0.01 cm^{-1}, the lines were remeasured and the erroneous readings were deleted. The errors due to (IV) were allowed for by adding the "dynamic pen separation" to the measured positions of the lines and the fringes. Factors (I-IV) also affect the accuracy of the fiducial constant A (and indirectly affect the accuracy of the wavenumbers of the spectral lines). From Eq. 2.5. and the usual laws of errors in a fraction[28], the error in the wavenumber was[18]

$$\sigma_1 = \left[(N_1\sigma_s/N_2)^2+(N_1 m\Delta A/N_c)^2+(A\Delta e_1/N_c)^2+(A\Delta e_2/N_c)^2\right]^{1/2} \quad 3.2.$$

where

σ_s is the error in the neon standard, usually of the order of 0.001 cm^{-1}

N_1 is the grating order of a line with wavenumber of σ_1

N_s is the grating order of a standard line.

m is the number of fringes between σ_1 and σ_s.

A is the fiducial constant.

e_1, e_2 } is the error in the fractional fringe count.

ΔA is the error in A.

N_c is the grating order of the continuous radiation.

N_1, N_s, N_c and m were usually of the order of 1, 3, 4 and 800 respectively. The error in the fractional fringe count (e_1 and e_2) was about 0.02. The error in the fiducial constant A was the difference in the two values of A calculated for each run and was of the order of 0.00001 cm^{-1}. The value of the fiducial constant A was of the order of 4.0 cm^{-1}. Substituting these values in Eq. 3.2., it can be seen that the first two terms on the right hand side of the equation can be neglected and the error in the wavenumber of a line can be of the order of 0.03 cm^{-1}. In practice, multiple observations have reduced this error to about 0.02 cm^{-1}. The low value of the actual error was obtained by comparing the wavenumbers of the neon lines recorded during a run, with the interferometrically measured values. Seventy-three neon lines, in various grating orders, were measured during the present project. The differences in the wavenumbers divided by the orders in which the lines were measured are shown in Fig. 3.1. The majority of differences lie within $\pm$ 0.02 cm^{-1}; none of the differences exceed $\pm$ 0.25 cm^{-1} which seems to be the largest inaccuracy. A further indication of the accuracy of the wavenumbers of the hafnium lines can be obtained by comparing the average values of the wavenumbers of the neon lines measured more than twice, with the interferometric values. The wavenumbers of eleven neon lines were measured more than twice; the arithmetic means and the root mean square

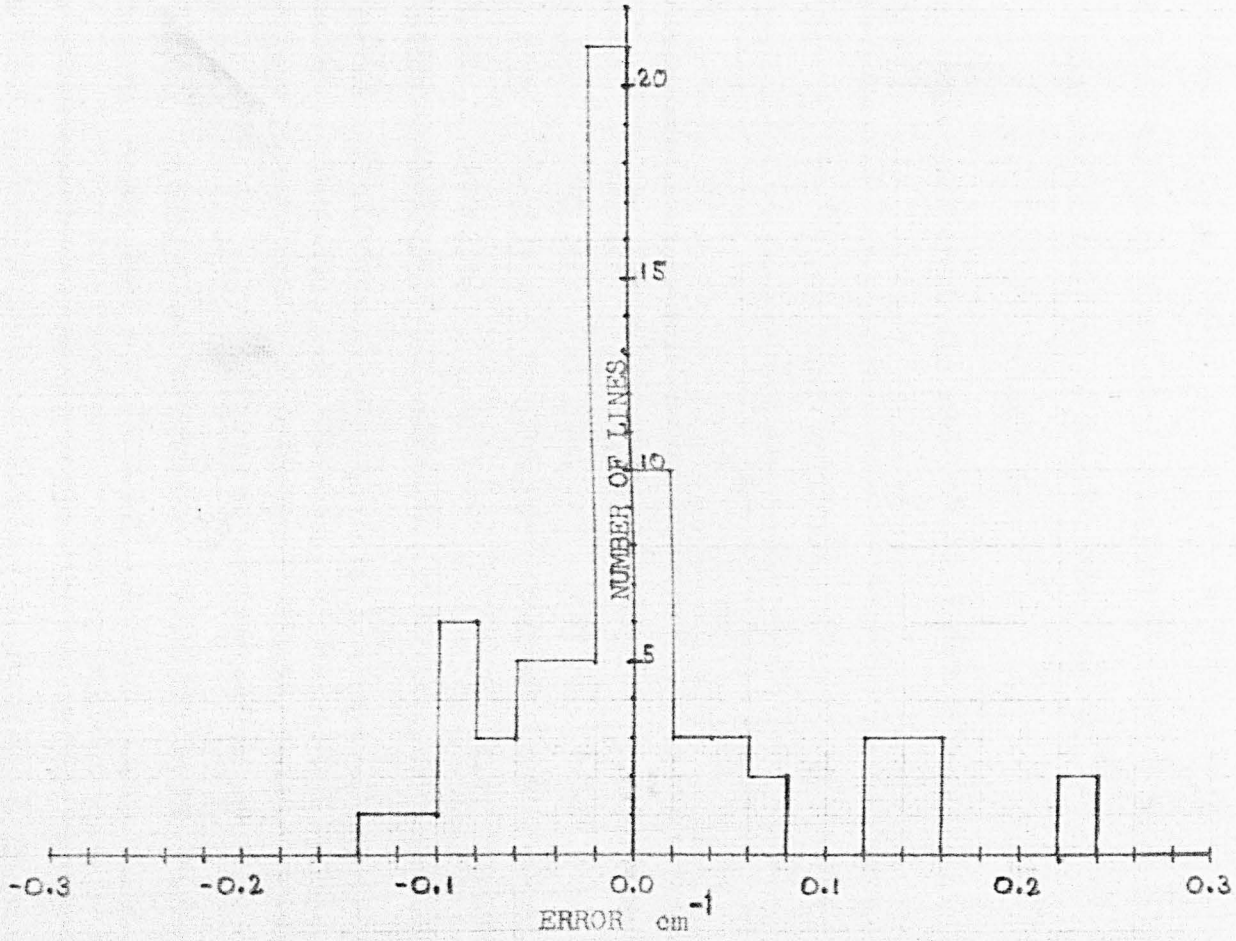

Fig. 3.1.

HISTOGRAM OF THE ERRORS OBSERVED IN THE WAVENUMBERS OF THE NEON LINES.

errors are given in Table 3.2. The wavenumbers measured by the two methods agree well within the limits of accuracy.

The large number of lines (86) which could be assigned to the energy levels of Hf I within an accuracy of 0.02 cm^{-1}, seemed to rule out any systematic errors due to (V) and (VI). The correction necessary for error (VI) could not be estimated as the data on temperature, pressure and humidity in the laboratory were not available but it has been shown[29] that this error was unlikely to be greater than 0.01 cm^{-1}.

TABLE 3.2.

Mean values and the rms. errors in the neon lines

λ_I	σ_I	ORD	$\sigma_I/ORD=\sigma'$	σ_m	Δ	$\sigma'-\sigma_m$
A	cm^{-1}		cm^{-1}	cm^{-1}	cm^{-1}	cm^{-1}
9665.424	10346.158	2	5173.079	5173.12	0.04	0.04
8783.755	11384.653	2	5692.327	5692.34	0.05	0.01
5852.4880	17086.750	3	5695.583	5695.60	0.11	0.01
5852.488	17086.750	4	4271.688	4271.74	0.04	0.06
6678.2766	14973.923	3	4991.308	4991.40	0.03	0.09
6074.3377	16462.700	4	4115.675	4115.67	0.01	0.00
11614.200	8610.150	1	8610.150	8610.19	0.06	0.04
6506.5278	15369.180	2	7684.592	7684.41	0.06	0.18
8495.3590	11771.133	2	5885.567	5885.59	0.08	0.03
8418.4274	11878.703	2	5959.352	5939.39	0.09	0.04
7032.4134	14219.869	2	7109.935	7110.09	0.11	0.16

where

λ_I is the interferometrically measured air wavelength

σ_I is the interferometrically measured air wavenumber

ORD is the grating order in which the lines were observed

σ_m is the mean value of the neon line wavenumber

Δ is the root-mean-square error in σ_m.

In Table 3.3., the hafnium lines in the wavelength region 1.0 - 1.20 μm have been compared with the wavenumbers of the same lines measured by Corliss et. al.[16]. The majority of lines agree within ± 0.05 cm^{-1} and practically all lines agree within 0.1 cm^{-1}. Only three lines (11219 Å, 11296 Å and 11602 Å) differ by as much as 0.2 cm^{-1} but the relative intensities of these three lines differ considerably in these two records. Two of these lines (11219 Å and 11296 Å) were relatively weak and have been assigned the accuracy code D (Table 3.4.) and errors of 0.1 - 0.2 cm^{-1} were likely in the present measurement. The discrepancy in the third line cannot be accounted for as the wavenumber measured during the present project seems to be correct; this line has been assigned to energy levels of Hf I with an accuracy of better than 0.01 cm^{-1} (level assignments given at the end of Chapter 4). A number of weak lines (intensities 1 as reported by Corliss et. al.) were not observed during the present analysis and some weak lines (~~intensities of 2 or below~~) observed during the present analysis have not been reported by Corliss et. al.

In preparing the final line list, given at the end of Chapter 4, only the lines recorded on at least two charts were included. The comparison of two charts was necessary to eliminate the strong noise peaks measured as spectral lines. The wavenumbers of spectral lines in the final line list were obtained by averaging six values for strong lines and four values for weak lines (two from each of the three charts). The root-mean-square error (Δ) was calculated for each line and was used to denote the accuracy of the lines. The error code is given in Table 3.4.

All the lines lying well in the water-vapour absorption bands were assigned the code W as the accuracy of these lines was uncertain. The weak lines measured by linear interpolation between the strong lines were accurate only to ± 0.5 cm^{-1} and these lines have been assigned the code E

TABLE 3.3.

Mf I INFRA-RED LINES, THE PRESENT RESULTS AND THE RESULTS OF CORLISS et.al.

PRESENT RESULTS				CORLISS et.al.		
SIGMA	LAMDA	INT	QLT	LAMDA	INT	
cm^{-1}	Å			Å		Å
I	II	III	IV	V	VI	II-V
9976.74	10023.31	1	B	10023.30	2	0.01
9963.62	10036.51	90	A	10036.53	150	-0.02
9912.23	10088.55	20	C	10088.51	40	0.04
9897.21	10103.86	4	C	10103.88	15	-0.02
9889.05	10112.19	4	A	10112.20	10	-0.01
9866.48	10135.33	3	D	10135.30	6	0.03
9833.94	10168.86	110	C	10168.81	20	0.05
9796.41	10207.82	7	A	10207.78	8	0.04
9795.48	10208.79	3	C	10208.74	2	0.05
9777.88	10227.17	20	B	10227.18	20	-0.01
9746.99	10259.58	30	B	10259.67	10	-0.09
9668.74	10342.61	3	C	10342.55	3	0.06
9626.34	10388.16	10	D	10388.31	8	-0.15
9617.78	10397.41	230	B	10397.45	200	-0.04
9602.41	10414.05	1	C	10414.09	3	-0.04
9597.85	10419.00	4	D	10418.99	6	0.01
9593.52	10423.70	230	C	10423.78	400	-0.08
9573.80	10445.17	4	E	10445.17	7	0.00
9541.85	10480.15	200	A	10480.21	200	-0.06
9537.98	10484.40	2	B	10484.44	3	-0.04
9526.78	10496.73	1	A	10496.77	3	-0.04
9499.10	10527.31	20	B	10527.28	25	-0.03
9477.93	10550.83	10	B	10550.85	100	-0.02
9438.53	10594.87	50	B	10594.89	50	-0.02
9414.26	10622.18	6	A	10622.14	12	0.04
9403.06	10634.84	5	A	10634.81	5	0.03
9400.22	10638.05	330	B	10637.93	150	0.12
9291.36	10762.69	3	E	10762.68	3	0.01
9283.01	10772.37	30	A	10772.33	15	0.04
9215.18	10851.66	10	B	10851.65	6	0.01
9201.02	10868.36	40	C	10868.44	20	-0.08

TABLE 3.3.(cont.)

I	II	III	IV	V	VI	II-V
9173.50	10900.96	2	B	10900.75	15	0.01
9162.09	10914.54	20	B	10914.47	50	0.07
9154.66	10923.40	6	B	10923.38	2	0.02
9145.95	10933.80	20	A	10933.82	10	-0.02
9142.29	10938.18	20	B	10938.08	2	0.10
9129.70	10953.26	8	C	10953.12	4	0.14
9114.46	10971.58	380	C	10971.61	50	-0.03
9090.88	11000.04	7	A	11000.00	3	0.04
9066.05	11030.16	50	A	11030.13	20	0.03
9058.77	11039.03	20	D	11039.01	4	0.02
9052.23	11047.00	80	D	11046.97	40	0.03
9029.76	11074.49	40	B	11074.42	5	0.07
9015.06	11092.55	3	C	11092.58	1	-0.03
8977.41	11139.07	80	C	11139.05	20	0.02
8936.48	11190.09	2	D	11190.17	1	-0.08
8913.41	11219.05	10	D	11219.28	1	-0.23
8906.52	11227.75	230	A	11227.70	10	0.05
8905.52	11228.99	460	D	11229.01	15	-0.02
8894.99	11242.28	40	B	11242.16	3	0.12
8851.94	11296.96	9	D	11296.74	1	0.22
8846.80	11303.52	100	C	11303.44	10	0.08
8798.91	11364.98	610	D	11365.02	25	-0.04
8777.19	11393.17	10	A	11393.12	1	0.05
8710.31	11480.65	200	A	11480.61	15	0.04
8618.93	11602.38	130	C	11602.16	4	0.22
8498.43	11766.88	150	B	11766.95	10	-0.07
8360.57	11960.91	390	B	11960.80	2	0.11
8303.55	12043.04	680	A	12043.08	6	-0.04

and their air wavelengths have been given only to the nearest angstrom. The lines recorded during the irregularities in the grating or the chart drive were also assigned the code E.

TABLE 3.4.

Accuracy Code

RMS Error Limit	Error Code
$0 = \Delta \leqslant \pm 0.02$ cm^{-1}	A
$\pm 0.02 < \Delta \leqslant \pm 0.05$ cm^{-1}	B
$\pm 0.05 < \Delta \leqslant \pm 0.10$ cm^{-1}	C
$\pm 0.1 < \Delta \leqslant \pm 0.2$ cm^{-1}	D
$\pm 0.2 < \Delta \leqslant \pm 0.5$ cm^{-1}	E

3.3. Measurement of Intensities

The calibration fringes were not necessary when the intensities of the hafnium lines were measured and the "folded" optical system used to measure the wavenumbers of the spectral lines was modified. The microwave source was mounted on an optical bench at I (Fig. 2.7.) and the light beam was focussed on the entrance slit by the concave mirror CM_2. This optical system made the entrance slit optics easier to adjust and had the additional advantage of improving the image quality. The light guide used to conduct the "calibration beam" to the photomultiplier was removed and the 2 cms length of the slits was used for the spectral beam. The light beam was chopped by a sectored disk rotated immediately in front of the source. The peak intensities of the spectral lines were measured by having an entrance slit of 175 μm width and an exit slit of 55 μm width to record uniform flat-topped line profiles throughout the 1.0 - 2.5 μm spectral range.

The linearity of the amplifier was tested by replacing the microwave excited source by a Phillips tungsten ribbon standard lamp (type W2KGV11).

The black-body emissions of the lamp at a particular wavelength and for different filament temperatures were plotted against the corresponding recorder deflections. The true temperature of the filament of the lamp was obtained from curves (supplied by Phillips) of filament current against filament temperature. The filament current was measured with a standard ammeter, the current being drawn from a stabilised current supply (Farnell Stabilised Current Supply - S series). The "linearity curves" were obtained for two amplifier gains and at two wavelengths. The black-body emission of the filament was not corrected for the transmission through the quartz envelope of the lamp as the 93% transmission factor was known to be constant between 1.0 - 3.0 μm spectral range. The amplifier was sufficiently linear (Fig. 3.2.) to measure intensities if allowance was made for 0.2 cms error in the pen recorder deflection.

The intensities of the hafnium lines were measured from only one chart recorded at each grating setting. The spectra were recorded after the hafnium lamp had been allowed to warm-up for about half an hour. The lead sulphide cell current was maintained at a constant value of 25 μA by interrupting the runs at one hour intervals to replenish the solid carbon dioxide used to cool the cell. The microwave power input and the reflected power were also kept constant. The regions of high water vapour absorption were bypassed during intensity measurements, as in this spectral region no meaningful indication of line intensities was possible using apparatus open to air. The heights of the tops of the line profiles were measured with an accuracy of 0.1 cms; the average background level in the immediate neighbourhood of the lines was used as a reference level.

The intensities of the hafnium lines were put on a uniform scale by correcting for the varying wavelength response of the lead sulphide cell. The wavelength response was corrected for by replacing the microwave excited source by the standard lamp. The black-body emission of the tungsten

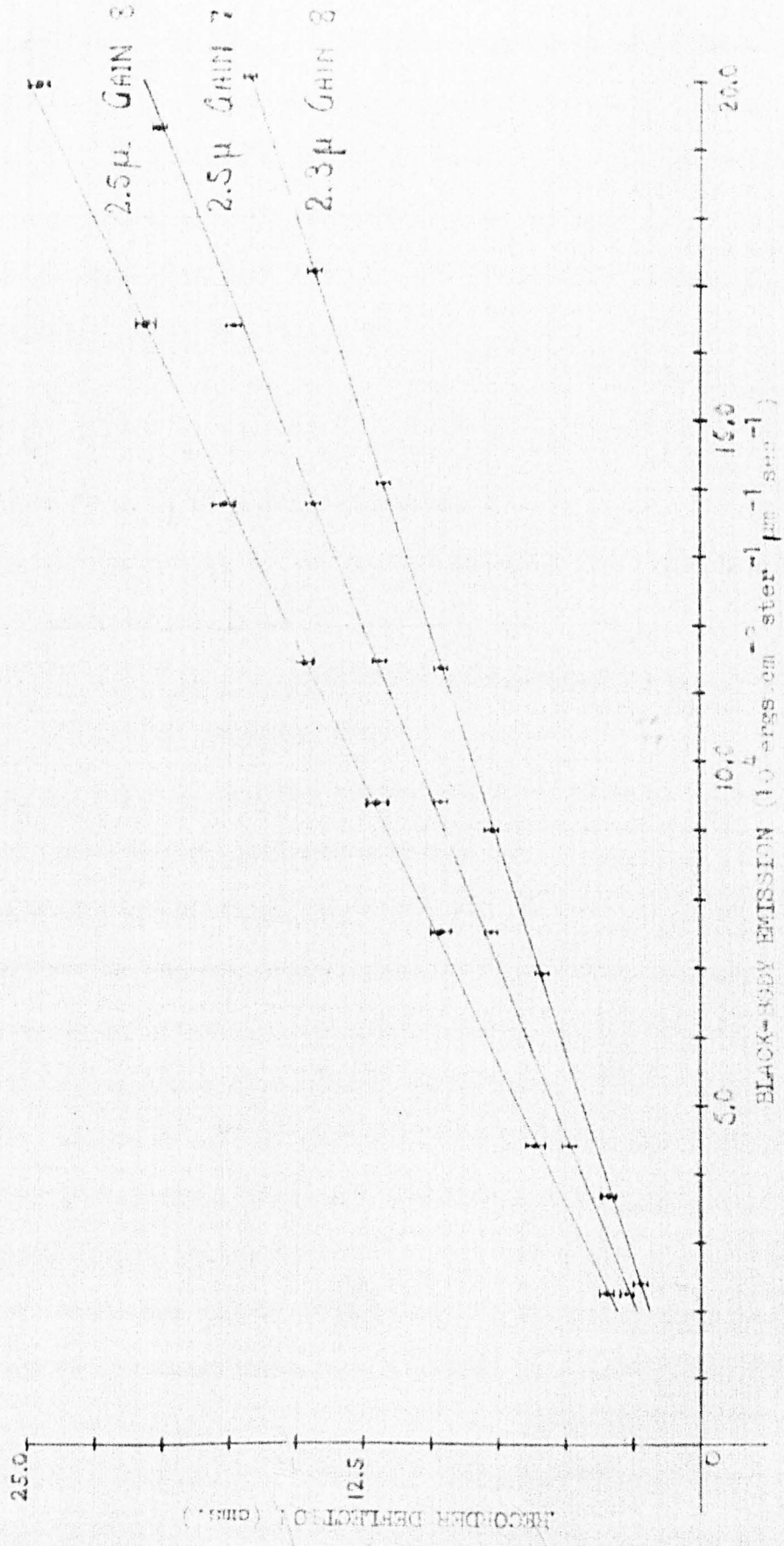

Fig.3.2. LINEARITY CURVES

filament kept at a constant temperature was recorded at 0.1 μm intervals. The back-ground level in this case was obtained by blocking the light beam at the entrance slit. A fourth-order polynomial was fitted to the pen-recorder deflections and the black-body emissions by the method of least squares[27,28], to obtain curves of wavelength against black-body emissions and of wavelength against pen-recorder deflections (Fig. 3.3. a,b). The polynomial relations were used to put the hafnium line intensities on a uniform scale using the relation

$$I_1 = D_1 \times (B_o + B_1\lambda + B_2\lambda^2 + B_3\lambda^3 + B_4\lambda^4)/(H_o + H_1\lambda + H_2\lambda^2 + H_3\lambda^3 + H_4\lambda^4) \qquad 3.7.$$

where I_1 is the hafnium line intensity

D_1 is the height of the top of the line profile above the back-ground level

B_i ($i = 0 - 4$) are the parameters for wavelength against black-body emission curve

H_i ($i = 0 - 4$) are the parameters of wavelength against pen-recorder deflection curve.

The height D_1 was obtained by correcting the height of the recorded line profile for the amplifier gain and for the external attenuation. The intensity of the weakest line was set equal to 1 and the intensities of the rest of the lines were scaled accordingly.

The different rate of change of the pen-recorder deflection in recording the spectral lines and the standard lamp emissions could have introduced errors in the intensities but the limit of accuracy of the measured values was set by uncertainty in the reference background level. The error in the intensities was believed to be about 10% and no corrections were made for the 1% increase in the line intensities observed after six hours of continuous operation of sources. The error in the back-ground level due

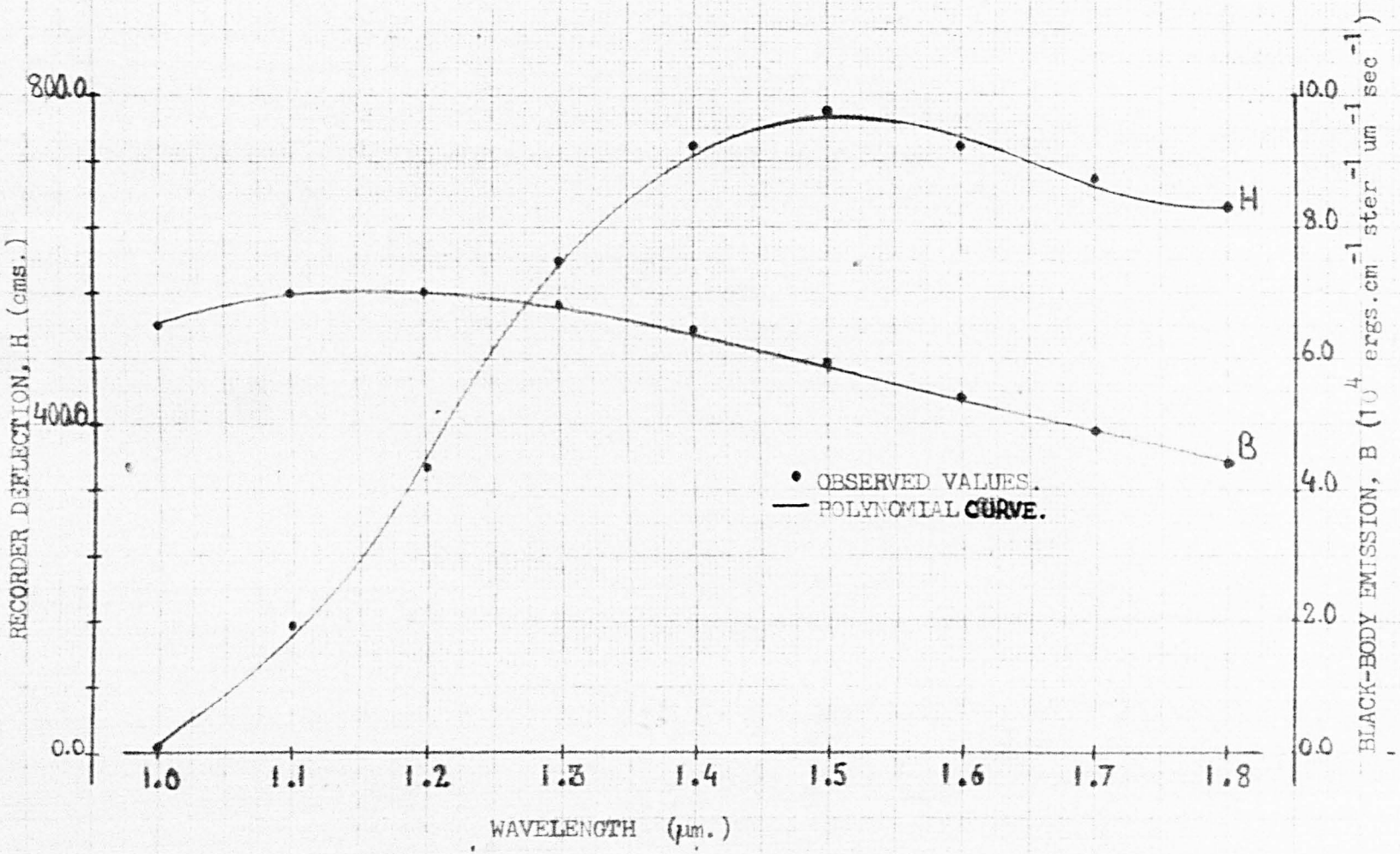

Fig. 3.3.a.

THE PEN RECORDER DEFLECTION AND THE BLACK-BODY EMISSION AS A FUNCTION OF THE WAVELENGTH.

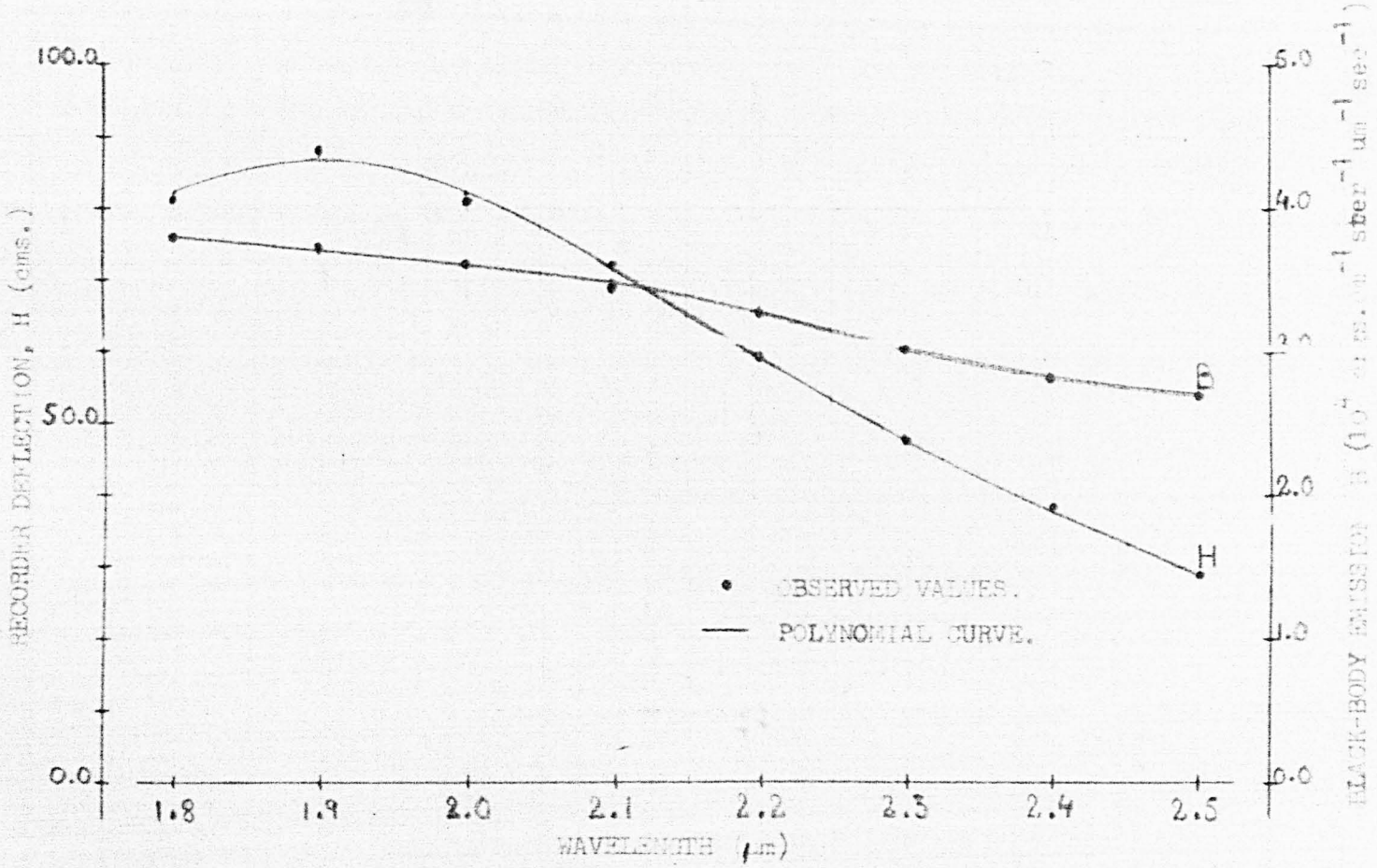

Fig. 3.3.a.

THE PEN RECORDER DEFLECTION AND THE BLACK-BODY EMISSION AS A FUNCTION OF THE WAVELENGTH

to the scattered light from the standard lamp was also ignored. The temperature characteristics of the discharge were not known and it was not possible to correct the intensities for self-absorption of the spectral lines. It is shown in the next chapter that the measured intensities were sufficiently accurate to aid the classification of lines.

CHAPTER 4

DATA ANALYSIS

The 521 hafnium lines observed in the 1.0 - 2.5 μm spectral range have been given in the line list at the end of this chapter. The line list includes in the columns:-

1. The observed air wavenumber.
2. The corresponding air wavelength.
3. The vacuum wavenumber.
4. The intensity of the lines.
5. The accuracy of the lines according to the code given in Table 3.4.
6. The quality of the lines.
7. The even energy levels of the possible transitions.
8. The J-quantum number of the even level.
9. The odd energy levels of the possible transitions.
10. The J-quantum numbers of the odd levels.
11. The calculated vacuum wavenumbers.
12. The difference between the calculated and the observed wavenumbers.

TABLE 4.1.

The Accuracy of Lines

Number of Lines	Accuracy
110	A
139	B
123	C
52	D
93	E

4.1. Classification of Lines

A computer programme (Appendix 2.1.) in Algol was designed to fit the observed hafnium lines to the energy levels of hafnium listed by

Moore (1958)[32]. The line fitting program differenced a pair of odd and even energy levels which satisfied the J-selection rule, and compared the calculated wavenumber with the wavenumbers of the observed lines. The observed wavenumber which agreed within a given error limit with the calculated wavenumber was printed along with the energy levels as possible transitions. The number of accidental coincidences in the line fitting program increased with the increase in the number of lines and with the decrease of accuracy of fit. The error limit was kept low (i.e. high accuracy of fit) when the number of lines was high. The lines fitted at a particular error limit were deleted from the line list before attempting to fit the remainder of the lines at a higher error limit (i.e. lower accuracy of the fit). The number of accidental coincidences was kept low by decreasing the total number of lines as the error limit was increased. The level fitting program was started with 470 hafnium lines; only lines whose wavenumbers were measured from charts which had calibration fringes recorded on them were included in the program. The weak lines measured by linear interpolation between the strong lines were not included in the level fitting program as the low accuracy of these lines would have increased the number of accidental coincidences. The accuracy limits, the total number of lines used and the number of lines assigned are given in Table 4.2.

The error limit as high as 0.1 cm^{-1} was used as the average accuracy of infrared lines was 0.05 cm^{-1} and the accuracy of the energy levels was believed to be 0.05 cm^{-1}. The accuracy of the energy levels was obtained by fitting the visible and near ultra violet lines to the energy levels; the maximum difference between the observed and the calculated wavenumbers was 0.05 cm^{-1}. Since the accepted energy levels were obtained from the visible and near ultra violet lines[32], the accuracy of the levels was assumed to be 0.05 cm^{-1}.

TABLE 4.2.

Accuracy Limits and Assigned Lines

Accuracy Limit	Number of Spectral Lines Used	Number of Lines assigned
$\pm$ 0.02 cm^{-1}	470	86
$\pm$ 0.05 cm^{-1}	384	72
$\pm$ 0.10 cm^{-1}	312	62

The accidental coincidences in the assigned lines could not be traced, but the intensities of the lines observed in transitions involving the term designated levels were used to verify the level assignments. In Table 4.3., the lines observed in the transitions $5d^3(^4F)6s\,^5F \rightarrow 5d^3 6s(^4F)6p\,^5F^\circ$ and $5d^3(^4F)6s\,^5P \rightarrow 5d^2 6s(^4F)6p\,^5D^\circ$ have been shown. The spectral lines in these two multiplets fall in the 1.0 - 2.5 μm region and the intensities of these lines were measured and put on a uniform scale. In Table 4.3. the air wavenumbers of the lines, the intensities of the lines, the quantity SE $\left[= (\text{Intensity})/(\text{Wavenumber})^4 \right]$ and the theoretical line strengths[37] have been listed. The intensities were found to obey the following rules for intensities of lines in multiplets[36];

1. The strongest lines are those for which the change in J is the same as that in L - Principal lines.
2. The strongest principal line is one with the largest J of the initial level. The intensities of the principal lines decrease with decreasing J.
3. Of the remaining lines, the lines in which the change in J is opposite to change in L are weaker than the lines in which the change in J is the same as that in L.

The line assignments in these multiplets seem to be correct. The intensity rules have been used to verify line assignments in transitions

TABLE 4.3.

THE RELATIVE LINE INTENSITIES AND THE LINE STRENGTHS IN THE MULTIPLETS OF Hf I

$5d^2 6s(^4F)6p\ ^5F^o$

	E(cm^{-1})	J	21738.70 1	22450.56 2	23448.61 3	24785.23 4	26202.53 5	
$5d^3(^4F)6s\ ^5F$	14092.28	1	7648.59	8360.57				W
			573	389				I
			100	48				SE
			20.2	10.1				ST
	14740.68	2	7000.16	7711.97	8710.31			
			*	575	201			
				97	21			
				25.3	15.2			
	15673.33	3		6779.18	7777.41	9114.46		
				78	578	382		
				22	94	33		
				15.2	39.8	15.8		
	16766.60	4			6683.83	8020.85	9438.53	
					143	657	50	
					43	95	4	
					15.8	64.0	11.1	
	17901.28	5				6885.83	8303.55	
						129	676	
						34	85	
						11.1	100	

$5d^2 6s(^4F)6p\ ^5D^o$

	E(cm^{-1})	J	24966.78 0	25194.47 1	25634.21 2	26305.78 3	27516.41 4
$5d^3(^4P)6s\ ^5P$	20784.87	1	4183.12	4410.90	4850.69		
			12	30	31		
			48	96	68		
			11.1	25.0	19.4		
	20908.42	2		4287.24	4727.04	5398.83	
				10	41	*	
				36	100		
				8.3	32.4		
	22199.08	3			4107.83	5318.88	
					6	*	
					26		
					25.9		

KEY

E Wavenumbers of the levels of the configuration.
J Total angular momentum quantum number of the level.
W Air wavenumber of the spectral line.
I Intensity of the spectral line.
SE Experimental line strength.
ST Theoretical line strength.
* The intensities of the lines marked with an asterisk were not measured.

involving classified terms. A number of infrared lines necessary to complete some of the transition arrays have been observed; the comparison of the intensities in such cases have not been unambiguous as the intensities of the visible lines occurring in the transition arrays were not on a uniform scale.

The low lying levels (especially those of the even terms) of hafnium appear to be LS-coupled as the level separations seem to follow the Landè interval rule[36]. The quanti ty S which is approximately equal to the line strength can, therefore, be compared with the theoretical multiplet line strengths given by White and Eliason (1933)[36,37]. In Table 4.8., the largest value of S has been set equal to 100; the other values have been sharply rounded off to make comparison with calculated line strengths easier. The experimental line strengths were not obtained as the temperature characteristics of the hafnium iodide sources was not studied during the present analysis of the hafnium spectrum and it was not possible to establish if an "excitation temperature" could be used to describe the population of the energy levels. The extent of self-absorption of the spectral lines was also unknown. Allowing for 10% error in the line intensities, the quantity SE agrees reasonably well with the theoretical line strengths except for lines lying along the principal diagonal. This lack of perfect agreement may be due to the absence of the corrections for the finite temperature of the source and the corrections for the self-absorption of spectral lines. The lack of agreement could also be due to the departures from perfect LS-coupling and the configuration interaction which would affect the intensities of the lines more than it would affect the level spacing.

The lines assigned to the classified levels appeared to be correct and it seemed reasonable to assume that lines assigned to levels for which only

the J quantum numbers were known were also correct. Only one line out of the 220 lines classified during the present project could be assigned to two pairs of levels. The spectral line and the two pairs of levels are given in Table 4.4. It was impossible to decide between either transitions and this line has been listed as an unclassified line.

Only one infrared hafnium line could be assigned to the energy levels of Hf II although some strong Hf II lines were possible in the 1.0 - 2.5 μm region. The accuracy of the fit was 0.05 cm^{-1} and the assignment was probably accidental. The absence of Hf II lines was also indicated by the lack of change in the relative intensities of lines in the spectra recorded at different microwave powers.

TABLE 4.4.

Two Possible Transitions

Wavenumber		Energy Levels				Wavenumber	O-C
(Air)	(VAC)	Even	J	Odd	J	(Calc)	
9201.02	9198.50	25678.60	3	34877.04	3	9198.44	-0.06
9201.02	9198.50	47606.21	2	38407.80	3	9198.41	-0.09

The presence of large numbers of unclassified lines - some quite strong - seemed to suggest that there could be energy levels which had not been found before. A level searching program[38,39,40] was designed to look for new levels. The level searching program calculated all the combinations - (level + line) and (level - line) - which were greater than zero. The levels were arranged in a descending order and "chains" of repeating combinations, within 0.25 cm^{-1}, were printed out. The number of fortuitous combinations to be expected by Poisson distribution and within a tolerance less than 0.25 cm^{-1} were also calculated. The number of fortuitous combinations are given by[40]

$$K = M\left[x^{N-1}/(N-1)!\right]e^{-x} \qquad 4.1.$$

where M is the number of combinations within a tolerance t

less than 0.25 cm^{-1}.

N is the number of combinations within 0.25 cm^{-1}.

$x = t.N/0.25$.

A single combination repeated four times within 0.25 cm^{-1} was found with all the unclassified lines used in the level searching program. The lines and the odd levels which combine to give the repeated combination are given in Table 4.5.

TABLE 4.5.

Combination	A Possible New Level Line Wavenumbers			Odd Energy Levels	
cm^{-1}	(Vac)	cm^{-1}	(Air)	cm^{-1}	J
22210.32	9400.48		9403.06	31610.80	2
22210.34	7786.47		7788.60	29996.81	3
22210.37	8192.54		8194.78	14017.83	1
22210.41	7775.28		7777.41	14435.13	2

The number of fortuitous combinations to be expected within a tolerance of 0.05 cm^{-1} was small ($K \simeq 0.1$). The combination 22210.34 cm^{-1} was probably a new even level ($J = 2$), although it was not possible to be certain as the number of repeated combinations was so small. The value of this combination was low enough for it to be a possible level of the low even configuantions of Hf I and a theoretical calculation of the positions of the energy levels of the low even configurations was necessary to classify the combination found above. The calculation of the energy levels is given in the next section.

4.2. Theoretical Calculation of the Energy Levels

The configurations $5d^26s^2$, $5d^36s$ and $5d^4$ probably form the low even configurations of Hf I[48] and the possible low level found in the last section was probably a level of one of these configurations. The positions of the energy levels of these configurations were calculated assuming both the electrostatic and the spin-orbit interactions.

In the central field approximation, the energy states of a configuration of an atom are given by the eigenvalues of energy matrices (one matrix for each possible value of the total angular momentum)[36,43]. The matrix elements connecting states b and b' may be written in the form[43,44]

$$H_{bb'} = E_{av}\delta_{bb'} + \sum_i \left[f_k F^k(l_i l_j) + g_k G^k(l_i l_j) \right] + \sum_i d_i \zeta(l_i) \qquad 4.2.$$

if only the electrostatic and the spin-orbit interactions are included. The l_i and l_j are the orbital angular momentum quantum numbers of a configuration of incompletely filled subshells. The E_{av} is the weighed average energy of all states of a configuration defined as,

$$E_{av} = \sum_i I_i(nl) + \sum (pair) E' \qquad 4.3.$$

where the single electron integral

$$I(nl) = \int_0^\infty r^{2l+1} \times \frac{d}{dr}\left(\frac{R^*_{nl}}{r^l}\right) \frac{d}{dr}\left(\frac{R_{nl}}{r^l}\right) - 2ZrR^*_{nl}R_{nl} \, dr \qquad 4.4.$$

where

Z is the atomic number of the atom

R_{nl} is the radial portion of the one electron wavefunction.

In Eq. 4.3., E' is the average interaction energy of pairs of electrons in the incompletely filled subshells and is made up of combinations of radial integrals F^k and G^k.

The Coulomb, exchange and spin-orbit interaction parameters (F^k, G^k and ζ respectively) are defined in terms of the radial portions

$R_{li}(r)$ of the one electron wavefunction,

$$F^k(l_i l_j) = \int_0^\infty \int_0^\infty R^*_{li}(r_1) R^*_{lj}(r_2) R_{li}(r_1) R_{lj}(r_2) \frac{2r_<^k}{2r_>^{k+1}} r_1^2 r_2^2 \, dr_1 dr_2 \qquad 4.5.a.$$

$$G^k(l_i l_j) = \int_0^\infty \int_0^\infty R^*_{li}(r_1) R^*_{lj}(r_2) R_{li}(r_2) R_{lj}(r_1) \frac{2r_<^k}{2r_>^{k+1}} r_1^2 r_2^2 \, dr_1 dr_2 \qquad 4.5.b.$$

$$\zeta(l_i) = \frac{\alpha^2}{2} \int_0^\infty R_{li}(r_i) \, R_{lj}(r_i) \left(\frac{dV}{dr_i}\right) r_i \, dr_i \qquad 4.5.c.$$

where

$r_<$ is the smaller of r_1 and r_2

$r_>$ is the larger of r_1 and r_2

$\alpha (= 1/137)$ is the fine structure constant

V is the potential due to the nucleus and the screening electrons.

The interaction parameters can be calculated if the radial portion of the one electron wavefunction is known (this can be calculated by the Hartree-Fock-Slater method). These parameters are commonly treated as empirically adjustable quantities to be determined by least-squares from the observed energy levels[45,46]. In Eq. 4.2., f_K, g_K and d_i are coefficient matrices which are functions only of the orbital angular momentum quantum numbers of the basic states b and b^1 in a chosen representation. General analytical methods for calculating the coefficient matrices have been developed by Racah[43,47].

The positions of the levels of the low even configurations ($5d^26s^2$, $5d^36s$ and $5d^4$) were calculated during the present project. The levels of the configuration $5d^26s^2$ have been identified[32] (except $^1S_0$), but not all the levels of the configuration $5d^36s$ and none of the levels of the configuration $5d^4$ are known. The large number of even levels for which no term designations had been made suggested that the levels of the

the configurations $5d^3 6s$ and $5d^4$ were represented. The term designations of the levels and the positions of unknown levels can be found by calculating the positions of the levels and comparing these with the observed levels[39,40]. The classified levels of the configuration $5d^2 6s^2$ of Hf I appeared to obey the Lande interval rule suggesting good LS-coupling in Hf I. However, the level schemes of the neighbouring atoms (Ta II, Z = 72[45] and Hf II, Z = 71[49]) indicated intermediate coupling to be better approximation.

The coefficient matrices in LS-coupling, of the electrostatic interaction within the configurations d^2s^2 and d^4 were obtained from tables compiled by Slater[43]. The electrostatic interaction matrices for the configuration d^3s were calculated from the matrices for the configuration d^3 by Dirac-Van Vleck's method of vector coupling. The coefficient matrices for the configuration d^3s are given by

$$E(d^3s) = E(d^3) - S_k \frac{G^2(sd)}{5} \quad \text{if } S = S_k + \tfrac{1}{2} \qquad 4.6.a.$$

$$E(d^3s) = E(d^3) + (S_k + 1) \frac{G^2(sd)}{5} \quad \text{if } S = S_k - \tfrac{1}{2} \qquad 4.6.b.$$

where

$E(d^3)$ is the diagonal component of the coefficient matrices of the configuration d^3.

S_k is the total spin quantum number of a multiplet of the configuration d^3.

S is the total spin quantum number of a multiplet of the configuration d^3s.

The spin-orbit interaction within a configuration d^n is given by[43]

$$(d^n vSLJ | \zeta(r_i) l_i . s_i | d^n vSLJ) = (-)^{S+L-J} (30)^{\frac{1}{2}} (d^n vSL \| V'' \| d^n vSL) W(SSLL;1J) \zeta(r_i) \qquad 4.7.a.$$

and the interaction within a configuration $d^n s$ is given by [50,51]

$$(d^n(vSL)sSLJ\,|\,\zeta(r_i)l_i.s_i|\,d^n(vSL)sSLJ)$$
$$(-)^{L-S-\frac{1}{2}-J}\,(30)^{\frac{1}{2}}\,(d^nvSL\|V^{11}\|d^nvSL)$$
$$[(2S\ 1)(2S\ 1)]^{\frac{1}{2}}\,W(SSLL;1J)\,W(ssss;\tfrac{1}{2}1)\,\zeta(r_i) \qquad \text{4.7.b.}$$

These relations were used to calculate the coefficient matrices for the spin-orbit interaction within the configurations $5d^4$, $5d^36s$ and $5d^26s^2$ (Appendix 1). In Eq. 4.7.a and b the reduced matrix elements $(d^n..... \| V^{11} \| d^n .....)$ were obtained from tables complied by Slater. The Racah function W(abed; ef) is a complicated function of the parameters a,b,c,d,e and f but reduces to simple functions for e equal to $\frac{1}{2}$ and 1 and for simple relations between a, b and c, d[52,53]. Tables of Racah functions for e equal to $\frac{1}{2}$ and 1 and for f = 0 to 6 for various combinations of a, b and c, d (e.g. b = a + 1, d = c - 1) were computed using the simple relations. The Racah functions encountered during the calculation of coefficient matrices of the spin-orbit interaction were reduced by symmetry relations of Racah functions to the tabulated functions.

The energy matrices were calculated using the following radial parameters:-

E_{av}	the weighes average energy of the configurations
$F^2(d,d)/441$	the Slater coulomb interaction
$F^4(dd)/441$	parameters
$G^2(ds)/10$	the Slater exchange interaction parameters for the configuration $5d^36s$
ζ	the spin-orbit interaction parameter.

The calculations were performed by the method described by Racah[46] and shown in the flow diagram of Fig. 4.1. As a first approximation the parameters ($F^2/441$, $F^4/441$, $G^2/10$ and ζ) of the configurations $5d6s^2$, $5d^26s$ and $5d^3$ of Hf II[49] were used to calculate the energy

matrices of Hf I. The weighed mean energy values E_{av} for the configurations $5d^2 6s^2$ and $5d^3 6s$ were calculated from the known energy levels of these configurations. The E_{av} for the configuration $5d^4$ could not be calculated as none of the levels of this configuration had been identified, and the parameter was estimated as follows. The configurations $5d^2 6s^2$, $5d^3 6s$ and $5d^4$ form the lowest even configurations of Ta II (Z = 72). The ratio

$$\frac{A(5d^4) - A(5d^3 6s)}{A(5d^3 6s) - A(5d^2 6s^2)}$$

(where A denotes the heights of the configurations as defined by Racah[47] for Ta II, (which equals 0.93) was set equal to the ratio

$$\frac{E_{av}(5d^4) - E_{av}(5d^3 6s)}{E_{av}(5d^3 6s) - E_{av}(5d^2 6s^2)} \qquad 4.8.$$

for Hf I to calculate $E_{av}(5d^4)$.

The energy matrices were diagonalised by the Jacobi-Naumann method[54,55] (Appendix 2). The eiganvalues of the energy matrices were compared with the known energy levels of the configurations and the parameters were improved by the method of least squares[43] (Appendix 2). The improved parameters were used for the next diagonalisation; the procedure was continued till the parameters converged. The final parameters were used to diagonalise the energy matrices; the eiganvalues and the Lande g-values calculated from the eiganvectors were output.

The results of the diagonalisation of the energy matrices of the configuration $5d^2 6s^2$ are given in Table 4.6. In column I the results obtained by using the known energy levels of the configuration $5d^2 6s^2$ to improve the interaction parameters are presented. The root-mean-square error (rms), defined as

$$\sigma = \left[\sum_i \Delta i/(n-m) \right]^{1/2} \qquad 4.9.$$

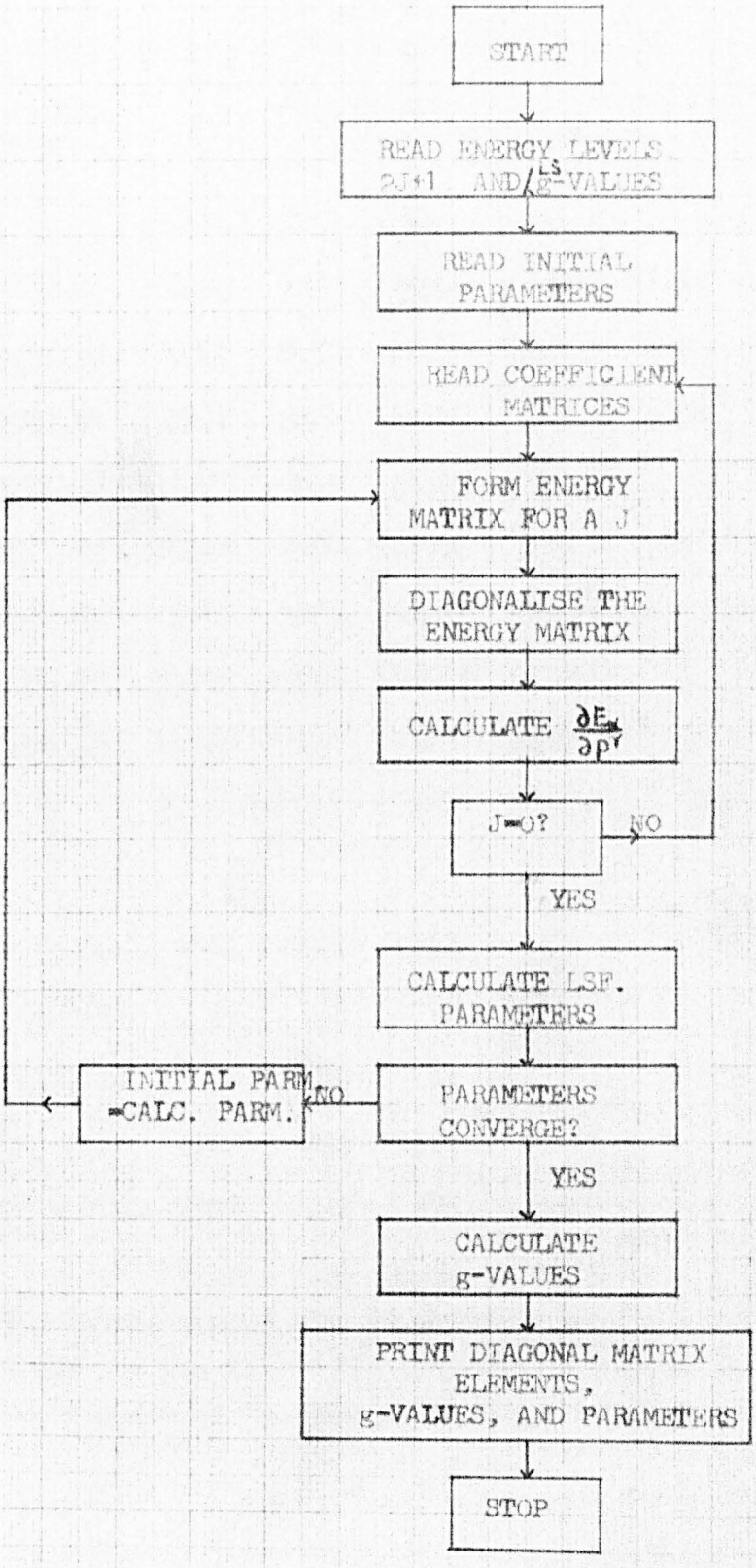

Fig. 4.1.

BLOCK DIAGRAM OF THE COMPUTER PROGRAM FOR CALCULATING THE ENERGY LEVELS, THE g-VALUES AND THE ATOMIC INTERACTION PARAMETERS.

TABLE 4.6.

ENERGY LEVELS OF THE CONFIGURATION $5d^2 6s^2$ OF Hf I

TERM	OBSERVED LEVEL cm^{-1}	CALCULATED LEVELS cm^{-1}				OBS-IV cm^{-1}	OBS g	CAL g
		I	II	III	IV		V	VI
$^3F_2$	0.0	-610	425	-550	199	-199	0.695	0.31
$^3F_3$	2356.68	1629	2053	1679	2428	71	1.083	1.08
$^3F_4$	4567.64	3871	3801	3919	4668	-100	1.240	1.18
$^3P_0$	5521.78	4976	4089	5149	5520	2	0.000	0.00
$^3P_1$	6572.55	6004	4764	6170	6541	31	1.500	1.50
$^3P_2$	8983.75	6245	5333	6399*	6670*		1.300	0.74
$^1D_2$	5638.75	10277	10504	10402*	11219*		1.165	0.45
$^1G_4$	10532.54	11148	11294	11319	10599	-66	1.008	0.94
$^1S_0$		27244*	29411*	27583*	27583*			0.96
$E_{av}(5d^2 6s^2)$		6142	6207	6253				
$F^2(dd)/441$		74	72	75				
$F^4(dd)/441$		74	93	74				
ζ		1228	933	1224				
σ		2386	1354	648	109			
		9.0%	5.0%	2.3%	0.4%			

* The levels marked with an asterisk were not included in the least squares fit of the interaction parameters and in the calculation of the root mean square errors.

where Δ_i is the difference between the observed and the calculated values of the energy levels

n is the number of equations used in the least squares fit

m is the number of parameters

is 2386 cm^{-1} i.e. 9% of the configuration width. The largest errors are in the values of the levels $^3P_2$ and $^1D_2$ and the energy values of these two levels probably need to be interchanged. However, a far more serious error appears to be in the values of the Coulomb interaction parameters F^2 and F^4. The "F^k - type" parameters are decreasing functions of k and it is rather strange that in the present calculation these two parameters should be equal. The results given in column II were calculated with the energy values of the levels $^3P_2$ and $^1D_2$ interchanged. The rms. error reduced to 5% of the configuration width, but judging from the values of F^2 and F^4 this calculation appears to be quite wrong. The results of column III were calculated assuming the energy levels $^3P_2$ and $^1D_2$ to be unknown; these levels were deleted from the least squares calculation by assigning a weight of zero to each. The rms.error in this calculation decreased to 2.3% of the configuration width and F^2 is slightly larger than F^4. The differences between the observed and the calculated values of the energy levels given in column III, follow a relation of the form (Fig. 4.2.)

$$\Delta E = 210 \left[L(L+1)\right] - 12.3 \left[L(L+1)\right]^2 \qquad 4.10$$

where

ΔE is the difference between the observed and the calculated values of the energy levels

L is the orbital momentum quantum number of the levels.

The rms.error between the observed and the corrected values of the energy levels was surprisingly low (0.4% of the configuration width).

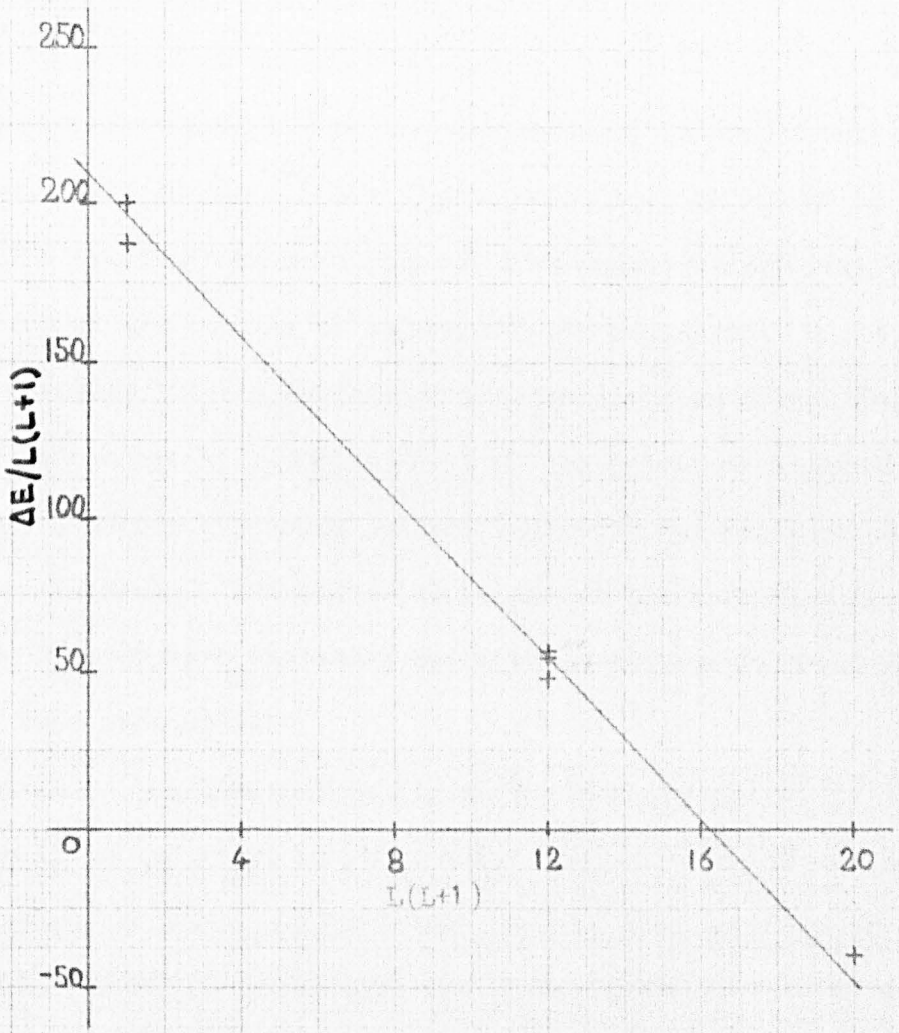

Fig. 4.2.

CORRECTION FOR THE ENERGY LEVELS OF THE CONFIGURATION $5d^2 6s^2$.

Trees[59] has suggested a correction proportional to $[L(L+1)]$ for the iron group of elements. This correction has been explained in terms of three-body interaction by Racah[60]. The correction of Eq. 4.10 does not seem to have been mentioned in the literature and it has not been possible to explain this correction in terms of atomic interactions. The correction may be due to the interaction with the neighbouring unknown levels or a higher approximation of the $[L(L+1)]$ correction. In column VI (Table 4.5) the Landè g-values calculated from eigenvectors obtained during the calculation of the results of column III are presented. The agreement between the observed and the calculated g-values is good except for levels with J = 2. The energy levels with J = 2 of the ground configuration are obviously very strongly perturbed and the energy values assigned to these levels seem to be wrong. The corrected values of the three levels $^3P_2$, $^1D_2$ and $^1S_0$ were used to obtain the exact positions of these levels but this has not been successful.

The results of the diagonalisation of the energy matrices of the configuration $5d^36s$ are given in Table 4.6. The positions of the levels obtained by using the known energy levels of this configuration in the least squares calculation of the parameters are given in column I. The rms error in this calculation is 408 cm^{-1} i.e. 1% of the configuration width. The Landè g-values are given in column II. The approximate positions of the energy levels given in column I were used to classify the even energy levels of Hf I by using the new and the old levels in the least squares adjustment of the interaction parameters. A number of observed levels with energies close to the calculated positions of the energy levels were tried out and the calculations were repeated till the interaction parameters had physically meaningful values (i.e. F^2 greater than F^4) and the rms. error was minimised. The reults of this calculation are given in column III. Seven new levels

TABLE 4.3.

ENERGY LEVELS OF THE CONFIGURATION $5d^3 6s$ OF Hf I

TERM	J	OBSERVED LEVEL cm^{-1}	g-value	CALCULATED LEVEL cm^{-1} I	OBS-CAL II	g-value III	LEVEL cm^{-1} IV	OBS-CAL V	g-value VI
$5d^3(^4F)6s^5F$	5	17901.28	1.40	17032	869	1.30	17052	848	1.37
	4	16766.60	1.36	15871	859	1.35	16108	658	1.35
	3	15673.33	1.25	15504	169	1.24	15855	-182	1.24
	2	14740.68	1.00	15368	-627	1.00	15740	-999	1.00
	1	14092.28	0.00	15241	-1149	0.00	15647	-1555	0.00
$5d^3(^4F)6s^3F_1$	4	23252.81		23515	-262	1.16	23175	78	1.24
	3	22880.24		23684	-804	0.11	22969	-90	1.05
	2	23327.71	0.90	22772	-434	0.66	22651	676	0.66
$5d^3(^4P)6s^5P$	3	22199.08		21332	867	0.17	20426	1773	0.17
	2	20908.42	1.74	21480	-572	1.37	20558	350	1.82
	1	20784.87		21254	-470	2.46	20376	409	2.49
$5d^3(^4P)6s^3P_1$	2			29003		1.37	27575		1.07
	1			28535		0.46	27480		0.24
	0			29135		1.00	27652		0.81
$5d^3(^2H)6s^3H$	6			25400		1.17	27513		1.06
	5			25321		0.96	27541		0.98
	4	27074.50*		25740		0.38	27772	-697	0.44

TABLE 4.3.(cont.)

			I	II	III	IV	V	VI
$5d^3(^2H)6s^1H$	5		29026		0.99	30906		1.00
$5d^3(^2G)6s^3G$	5	24085.14*	23690		1.03	26081	-1996	1.11
	4		22616		0.56	25403		0.61
	3	25678.60*	22746		0.08	25810	-131	0.72
$5d^3(^2G)6s^1G$	4		27211		0.87	29438		0.95
$5d^3(^2F)6s^3F_2$	4		30945		1.24	31889		1.24
	3	31054.64*	31033		1.07	31956	-901	1.07
	2	30146.40*	31069		0.66	31975	-1829	0.63
$5d^3(^2F)6s^1F$	3		34716		0.99	35397		1.00
$5d^3(^2D)6s^3D_1$	3		38459		0.19	41909		0.26
	2		38704		0.66	42063		0.91
	1	39286.19*	38692		0.27	42029	-2743	0.38
$5d^3(^2D)6s^1D_1$	2	41298.36*	42466		0.56	45568	-4270	0.78
$5d^3(^2D)6s^3D_2$	3		26159		0.19	28812		0.27
	2		26110		0.35	28777		0.82
	1		25819		0.19	28622		0.36

TABLE 4.8.(cont.)

		I	II	III	IV	V	VI
$5d^3(^2D)6s\,^1D_2$	2	29670		0.48	32150		0.73
$5d^3(^2P)6s\,^3P_2$	2	25077		0.98	27218		0.98
	1	25104		1.18	27203		0.18
	0	25112		1.00	27267		0.81
$5d^3(^2P)6s\,^1P$	1	29404		0.29	30986		0.95
$E_{Av}(5d^36s)$		25779			27144		
$F^2(dd)/441$		65			70		
$F^4(dd)/441$		40			66		
$G^2(ds)/10$		933			868		
ζ		242			180		
σ		408			1107		
		1%			2%		

* The levels marked with an asterisk were assigned during the present project.

were assigned to the configuration $5d^3 6s$. The rms error was 865 cm^{-1} i.e. 2% of the configuration width. The Lande g-values obtained during this calculation are given in column IV. The possible new level found in the last section falls in the energy range covered by the levels of the configuration $5d^3 6s$, but it has not been possible to classify this level.

The results of diagonalisation of the energy matrices of the configuration $5d^4$ are given in Table 4.8. The starting value of the parameter E_{av} was obtained from relation 4.8. given previously in this chapter. The interaction parameters F^2, F^4 and for the configuration $5d^3 6S$ were used to calculate the energy matrices. It was not possible to classify the known even levels of Hf I as the energy levels of the configuration $5d^4$ in order to determine the exact value of the interaction parameters of this configuration.

TABLE 4.8.

ENERGY LEVELS OF THE CONFIGURATION $5d^4$ OF Hf I

TERM	J	OBSERVED LEVEL cm^{-1}	g-value	CALCULATED LEVEL cm^{-1}	OBS-CAL	g-value
^5D	4			33122		1.49
	3			32892		1.50
	2			32673		1.45
	1			32477		1.34
	0			32349		0.82
	6			40075		1.15
	5			40012		0.99
	4			39855		0.76
^3G	5			42166		1.16
	4			42050		0.82
	3			41837		0.66
$^3P_1$	4			52360		0.76
	3			52437		0.61
	2			52418		0.36
$^3P_2$	4			41098		0.51
	3			41084		0.51
	2			41019		0.36
^3D	3			44672		1.32
	2			44629		1.13
	1			44713		0.50
$^3P_1$	2			58480		0.18
	1			58994		0.19
	0			59200		0.13
$^3P_2$	2			35209		0.15
	1			34538		0.08
	0			34220		0.01
^1I	6			43685		0.99
$^1G_1$	4			54958		0.32
$^1G_2$	4			44349		0.29
^1F	3			49360		0.97
$^1D_2$	2			62754		0.56
$^1D_1$	2			47157		0.53
$^1S_2$	0			66738		0.90
$^1S_1$	0			50987		0.91
		$E_{av}(d^4)$		43938		
		$F^2(dd)/441$		65		
		$F^4(dd)/441$		40		
		ζ		242		

THE INFRA-RED SPECTRUM OF HAFNIUM I

Key to Column Headings

1. air wavenumber
2. air wavelength
3. vacuum wavenumber
4. relative intensity
5. wavenumber precision: A, $\pm$ 0.02 cm^{-1}; B, $\pm$ 0.05 cm^{-1}
   C, $\pm$ 0.10 cm^{-1}; D, $\pm$ 0.20 cm^{-1}
   E $\pm$ 0.50 cm^{-1}
   W, wavenumber precision uncertain because of water vapour absorption bands
6. quality of line:
   - B broad
   - AS asymmetric
   - ASL asymmetric with suspected unresolved line on long wavelength side
   - ASS asymmetric with suspected unresolved line on short wavelength side
7. even energy level of possible transition
8. J quantum number of even level
9. odd energy level of possible transition
10. J quantum number of odd level
11. calculated wavenumber
12. difference between observed and calculated wavenumber.

PRESENT OBSERVATIONS						TRANSITIONS					
SIGMA (AIR) cm^{-1}	LAMDA (AIR) Å $^{-1}$	SIGMA (VAC) cm^{-1}	INT	ACC	QLT	LEVEL EVEN cm^{-1}	J	LEVEL ODD cm^{-1}	J	SIGMA (CAL) cm^{-1}	DIFF OBS-CAL cm^{-1}
(1)	(2)	(3)	(4)	(5)	(6)	(7)	(8)	(9)	(10)	(11)	(12)
9978.91	10021.13	9976.18	60	C							
9976.74	10023.31	9974.01	3	B		4567.64	4	14101.28	3	9930.04	-0.03
9963.62	10036.51	9960.89	90	A		15673.33	3	25634.21	2	9960.88	0.01
9927.66	10072.87	9924.94	20	B							
9917.85	10082.83	9915.13	3	C							
9915.75	10084.97	9913.03	3	C							
9912.23	10088.55	9909.51	23	C		24085.14	5	33994.71	4	9909.57	-0.06
9907.98	10092.87	9905.26	3	C							
9903.95	10096.98	9901.24	3	B							
9897.21	10103.86	9894.50	4	C		26715.37	3	36609.85	3	9894.48	0.02
9895.58	10105.52	9892.87	4	C							
9889.05	10112.19	9886.34	4	A		23252.81	4	33139.12	3	9886.31	0.03
9879.78	10121.68	9877.07	3	B							
9866.48	10135.33	9863.78	3	D		25084.14	2	34947.95	2	9863.81	-0.03
9849.67	10152.62	9846.97	20	D							
9833.94	10168.86	9831.25	110	C							
9810.77	10192.88	9808.08	10	A	B						
9796.41	10207.82	9793.73	7	A		23327.71	2	33121.48	2	9793.77	-0.04
9795.48	10208.79	9792.80	3	C							
9793.16	10211.21	9790.48	50	B							

(1)	(2)	(3)	(4)	(5)	(6)	(7)	(8)	(9)	(10)	(11)	(12)
9777.88	10227.17	9775.20	20	B		25678.60	3	35453.83	3	9775.23	-0.03
9762.57	10243.20	9759.90	60	A							
9746.99	10259.58	9744.32	30	B		22199.08	3	31943.31	4	9744.23	0.09
9683.35	10327	9680.70	3	E							
9668.74	10342.61	9666.09	3	C		25281.81	3	34947.95	2	9666.14	-0.05
9641.94	10371.36	9639.30	30	B	ASL						
9633.23	10380.73	9630.59	570	B							
9626.34	10388.16	9623.70	10	D		28527.97	1	38151.71	1	9623.74	-0.04
9617.78	10397.41	9615.16	230	B		17901.28	5	27516.41	4	9615.13	0.02
9613.36	10402.19	9610.73	10	C							
9609.06	10406.85	9606.43	760	C							
9602.41	10414.05	9599.78	1	C							
9597.85	10419.00	9595.22	4	D		25281.81	3	34877.04	3	9595.23	-0.01
9593.52	10423.70	9590.89	230	C		6572.55	1	16163.36	2	9590.81	0.01
9573.80	10445.17	9571.18	4	E							
9557.35	10463.15	9554.73	540	A	ASL						
9554.11	10466.70	9551.49	1	A							
9541.85	10480.15	9539.24	200	A		16766.60	4	26305.78	3	9539.18	0.06
9537.98	10484.40	9535.37	2	B		27074.50	4	36609.85	3	9535.35	0.02
9526.78	10496.73	9524.17	1	A		25281.81	3	34805.89	4	9524.08	0.09

(1)	(2)	(3)	(4)	(5)	(6)	(7)	(8)	(9)	(10)	(11)	(12)
9514.82	10509.92	9512.21	40	C		25084.14	2	34596.45	1	9512.31	-0.10
9499.10	10527.31	9496.50	20	B							
9497.94	10528.60	9495.34	20	D							
9493.24	10533.81	9490.64	130	A	AS						
9477.93	10550.83	9431.33	10	B							
9010*06	10577.47	9451.47	340	A							
9438.53	10594.87	9435.94	50	B		16766.60	4	26202.53	5	9435.93	0.01
9429.83	10604.65	9427.25	30	A							
9415.81	10620.44	9413.23	680	B	AS						
9414.26	10622.18	9411.68	6	A		22199.08	3	31610.80	2	9411.72	-0.04
9403.06	10634.84	9400.48	5	A							
9400.22	10638.05	9397.65	330	B		8983.75	2	18381.43	3	9397.68	-0.03
9385.98	10654.19	9383.41	4	A							
9364.51	10678.62	9361.95	8	A							
9348.67	10696.71	9346.11	5	B		41298.36	2	31952.25	1	9346.11	0.00
9314.46	10736.00	9311.91	7	C							
9312.53	10738.22	9309.98	7	C		23327.71	2	14017.83	1	9309.88	0.10
9291.36	10762.69	9288.82	3	E							
9283.01	10772.37	9280.47	30	A		23252.81	4	32533.30	3	9280.49	-0.02
9219.74	10846.29	9217.22	4	A							

(1)	(2)	(3)	(4)	(5)	(6)	(7)	(8)	(9)	(10)	(11)	(12)
9215.18	10851.66	9212.66	10	B	AS	31054.64	3	40267.35	2	9212.71	-0.05
9201.02	10868.36	9198.50	40	C							
9199.42	10870.25	9196.90	2	C							
9173.50	10900.96	9170.99	2	B		40513.55	2	31342.51	3	9171.04	-0.05
9162.09	10914.54	9159.58	20	B		8983.75	2	18143.37	1	9159.62	-0.04
9154.66	10923.40	9152.15	6	B	B						
9145.95	10933.80	9143.45	20	A		22199.08	3	31342.51	3	9143.43	0.02
9142.29	10938.18	9139.79	20	B		31054.64	3	40194.46	2	9139.82	-0.04
9129.70	10953.26	9127.20	8	C		25678.60	3	34805.89	4	9127.29	-0.09
9114.46	10971.58	9111.96	380	C		15673.33	3	24785.23	4	9111.90	0.06
9090.88	11000.04	9088.39	7	A		20908.42	2	29996.81	3	9088.39	0.00
9066.05	11030.16	9063.57	50	A		22880.24	3	31943.84	2	9063.60	-0.03
9058.77	11039.03	9056.29	20	D							
9052.23	11047.00	9049.75	80	D							
9029.76	11074.49	9027.29	40	B		8983.75	2	18011.05	2	9027.30	-0.01
9015.06	11092.55	9012.59	3	C							
8977.41	11139.07	8974.95	80	C							
8971.02	11147	8968.56	4	E							
8970.50	11147.65	8968.04	60	C		20784.87	1	29752.84	2	8967.97	0.07
8936.48	11190.09	8934.03	2	D							

(1)	(2)	(3)	(4)	(5)	(6)	(7)	(8)	(9)	(10)	(11)	(12)
8933.74	11193.52	8931.29	1	B		36523.84	3	45455.15	3	8931.31	-0.02
8923.27	11206.65	8920.83	6	C		25084.14	2	16163.36	2	8920.78	0.04
8913.41	11219.05	8910.97	10	D							
8906.52	11227.73	8904.08	230	A							
8905.52	11228.99	8903.08	460	D		5638.62	2	14541.68	3	8903.06	0.02
8899.59	11236.47	8897.15	40	B		47304.97	2	38047.80	3	8897.17	-0.01
8894.99	11242.28	8892.56	40	B		23327.71	2	14435.13	2	8892.58	-0.02
8851.94	11296.96	8849.52	9	D		27074.50	4	18224.99	4	8849.51	0.00
8846.80	11303.52	8844.38	100	C		20908.42	2	29752.84	2	8844.42	-0.04
8811.92	11348.83	8809.51	3	B	AS	35115.28	2	26305.78	3	8809.50	0.01
8798.96	11364.98	8796.55	610	D		5638.62	2	14435.13	2	8796.51	0.04
8796.48	11368.18	8794.07	610	D							
8786.20	11381.48	8783.80	3	B		44777.50	4	35993.70	5	8783.80	-0.01
8777.19	11393.17	8774.79	10	A		26918.14	1	18143.37	1	8774.77	0.01
8762.17	11412.70	8759.77	30	C							
8740.87	11440.51	8738.48	3	A		26715.37	3	35453.83	3	8738.46	0.01
8732.92	11450.92	8730.53	60	D		22880.24	3	31610.80	2	8730.56	-0.03
8731.75	11452.46	8729.36	3	A		35115.28	2	43844.63	1	8729.35	0.01
8715.47	11473.85	8713.08	30	B		25281.81	3	33994.86	2	8713.05	0.03
8713.52	11476.42	8711.14	10	B		23252.81	4	14541.68	3	8711.13	0.00

(1)	(2)	(3)	(4)	(5)	(6)	(7)	(8)	(9)	(10)	(11)	(12)
8710.31	11480.65	8707.93	200	A		14740.68	2	23448.61	3	8707.93	0.00
8695.25	11500.53	8692.87	7	D		40636.26	2	31943.31	4	8692.95	-0.08
8692.90	11503.64	8690.52	6	D		23252.81	4	31943.31	4	8690.50	0.02
8669.90	11534.16	8667.53	10	C		25281.81	3	33942.28	3	8667.47	0.06
8653.67	11555.79	8651.30	4	B		35115.28	2	26463.93	1	8651.35	-0.05
8650.04	11560.64	8647.67	5	C							
8648.13	11563.19	8645.76	5	C	AS						
8626.83	11591.74	8624.47	3	C		23327.71	2	31952.25	1	8624.54	-0.07
8618.93	11602.38	8616.57	130	C		20784.87	1	29401.44	2	8616.57	-0.10
8614.43	11608.43	8612.07	1	D							
8611.78	11612	8609.42	1	E							
8590.75	11640.43	8588.40	2	B		36523.84	3	45112.22	3	8588.38	0.02
8587.49	11644.85	8585.14	7	C		31119.20	2	39704.41	1	8585.21	-0.07
8577.26	11658.73	8574.91	10	C							
8543.65	11704.60	8541.31	4	D		43489.28	3	34947.95	2	8541.33	-0.02
8536.42	11714.51	8534.08	4	B		22199.08	3	30733.22	4	8534.14	-0.06
8528.65	11725.19	8526.32	4	C	B	34991.54	1	43517.85	2	8526.31	0.01
8525.79	11729.12	8523.46	4	B		42061.59	3	33538.15	2	8523.44	0.02
8498.43	11766.88	8496.10	150	B		5521.78	0	14017.83	1	8496.05	0.05
8495.33	11771.17	8493.01	70	B		20908.42	2	29401.44	2	8493.02	-0.02

(1)	(2)	(3)	(4)	(5)	(6)	(7)	(8)	(9)	(10)	(11)	(12)
8492.68	11774.85	8490.36	4	B		26715.37	3	18224.99	4	8490.38	-0.03
8488.98	11779.98	8486.66	7	B		38289.38	2	46775.98	3	8486.60	0.06
8476.57	11797.22	8474.25	1	C							
8464.55	11813.98	8462.23	6	D		22880.24	3	31342.51	3	8462.27	-0.04
8457.25	11824.17	8454.94	1	C							
8456.33	11825.46	8454.02	2	A		25084.14	2	33538.15	2	8454.01	0.01
8448.80	11836.00	8446.49	6	B	B						
8447.35	11838.03	8445.04	6	C		22880.24	3	14435.13	2	8445.11	-0.07
8440.74	11847.30	8438.43	4	B		40513.55	2	48951.97	2	8438.42	0.01
8423.64	11871.35	8421.34	2	B		28527.97	1	36949.29	1	8421.32	0.02
8411.51	11888.47	8409.21	10	C		28200.54	2	19791.30	2	8409.24	-0.03
8404.95	11897.75	8402.65	3	B		35115.28	2	43517.85	2	8402.57	0.08
8396.77	11909.34	8394.47	3	C		39127.61	3	30733.22	4	8394.39	0.08
8382.86	11929.10	8380.57	2	A		31054.64	3	39435.20	2	8380.56	0.01
8381.48	11931.07	8379.19	10	D		5638.62	2	14017.83	1	8379.21	-0.02
8369.64	11947.95	8367.35	8	B							
8368.53	11949.53	8366.24	8	C	B						
8360.57	11960.91	8358.28	390	B							
8340.85	11989.19	8338.57	30	A		22880.24	3	14541.68	3	8338.56	0.01
8336.52	11995.41	8334.24	2	C		42283.48	4	33949.28	3	8334.20	0.04

(1)	(2)	(3)	(4)	(5)	(6)	(7)	(8)	(9)	(10)	(11)	(12)
8318.28	12021.72	8316.00	40	A		31119.20	2	39435.20	2	8316.00	0.00
8313.04	12029.29	8310.77	20	A	B						
8309.30	12034.71	8307.03	7	A							
8304.71	12041.36	8302.44	20	C							
8303.55	12043.04	8301.28	680	A		17901.28	5	26202.53	5	8301.25	0.03
8285.33	12069.53	8283.06	7	B		23327.71	2	31610.80	2	8283.09	-0.03
8263.60	12101.26	8261.34	4	B	AS	30146.40	2	38407.80	3	8261.40	-0.06
8258.58	12108.62	8256.32	4	A		25281.81	3	33538.15	2	8256.34	-0.02
8247.09	12125.49	8244.83	3	B		28527.97	1	36772.85	2	8244.88	-0.05
8234.82	12143.56	8232.57	7	C		26715.37	3	34947.95	2	8232.58	-0.01
8213.36	12175.29	8211.11	5	A							
8201.84	12192.39	8199.60	3	B							
8194.78	12202.89	8192.54	3	C							
8180.24	12224.58	8178.00	2	C		40130.23	2	31952.25	1	8177.98	0.02
8163.91	12249.03	8161.68	3	C		26715.37	3	34877.04	3	8161.67	0.01
8161.42	12252.77	8159.19	3	B		41298.36	2	22139.12	3	8159.24	-0.05
8154.12	12263.74	8151.89	60	D							
8102.18	12342.36	8099.96	3	B							
8093.32	12355.87	8091.11	3	C							
8091.87	12358.08	8098.66	20	B	ASS	23252.81	4	31342.51	3	8098.70	-0.04

(1)	(2)	(3)	(4)	(5)	(6)	(7)	(8)	(9)	(10)	(11)	(12)
8086.70	12365.98	8084.49	3	C		31619.97	2	39704.41	1	8084.44	0.05
8082.26	12372.78	8080.05	2	A							
8076.95	12380.91	8074.74	3	B		31119.20	2	39193.91	3	8074.71	0.03
8069.05	12393.03	8066.84	1	D		42061.59	3	33994.71	4	8066.88	-0.04
8057.20	12411.26	8055.00	2	B		25084.14	2	33139.12	3	8054.98	0.02
8055.93	12413.22	8053.73	9	A		25084.14	2	33137.87	1	8053.73	0.00
8039.53	12438.54	8037.33	20	A		25084.14	2	33121.48	2	8037.34	-0.01
8030.02	12453.27	8027.82	2	C							
8020.85	12467.51	8018.66	660	A							
8016.96	12473.56	8014.77	1	B		23327.71	2	31342.51	3	8014.80	-0.03
8007.57	12488.18	8005.38	20	A		20784.87	1	28790.25	1	8005.38	0.00
7988.45	12518.07	7986.27	2	C							
7982.43	12527.51	7980.25	3	A		40513.55	2	32533.30	3	7980.25	0.00
7973.43	12541.65	7971.25	270	A		15673.33	3	23644.64	3	7971.31	-0.06
7941.64	12591.86	7939.47	4	A							
7883.71	12684.38	7881.55	1	C							
7864.45	12715.45	7862.30	210	D		48129.57	1	40267.35	2	7862.22	0.08
7860.28	12722.19	7858.13	70	D		24085.14	5	31943.31	4	7858.17	-0.04
7850.99	12737.25	7848.84	180	D	AS	10532.54	4	18381.43	3	7848.89	-0.05
7844.12	12748.40	7841.97	2	C	B	34991.54	1	27149.64	2	7841.90	-0.07

(1)	(2)	(3)	(4)	(5)	(6)	(7)	(8)	(9)	(10)	(11)	(12)
7818.00	12791	7815.86	1	E							
7803.99	12813.96	7801.86	3	A							
7788.60	12839.28	7786.47	10	E							
7777.41	12857.75	7775.28	580	B		15673.33	3	23448.61	3	7775.28	0.00
7762.09	12883.13	7759.97	3	A							
7726.26	12942.87a	7724.15	30	A		23252.81	4	30976.99	5	7724.18	-0.03
7711.97	12966.86	7709.86	580	A		14740.68	2	22450.56	2	7709.88	-0.02
7694.23	12996.75	7692.13	70	C							
7680.14	13020.60	7678.04	1	D	B						
7648.59	13074.31	7646.50	570	B		14092.28	1	21738.70	1	7646.42	-0.08
7619.86	13123.60	7617.78	9	C							
7605.01	13149.23	7602.93	80	B							
7562.91	13222.42	7560.85	190	C							
7555.91	13234.67	7553.84	3	C		22199.08	3	29752.84	2	7553.76	0.08
7509.95	13315.67	7507.90	1	B		47702.41	2	40194.46	2	7507.95	-0.05
7495.00	13340.45	7493.95	10	A		34991.54	1	42485.50	1	7493.96	-0.01
7495.83	13340.75	7493.78	2	B							
7486.84	13356.77	7484.79	5	B							
7462.88	13399.65	7460.84	2	D							
7455.93	13412.14	7453.89	2	B							

(1)	(2)	(3)	(4)	(5)	(6)	(7)	(8)	(9)	(10)	(11)	(12)
7447.66	13427.04	7445.62	430	B							
7312.44	13675.33	7310.44		W							
7303.20	13692.63	7301.20		W							
7282.54	13731.47	7280.55		W	ASL						
7273.03	13749.43	7271.04		W							
7251.94	13789.41	7249.96		W	AS						
7204.42	13880.37	7202.45		W		22199.08	3	29401.44	2	7202.36	0.09
7181.64	13924.40	7179.68		W		8983.75	2	16163.36	2	7179.61	-0.07
7166.38	13954.05	7164.42		W		23327.71	2	16163.36	2	7164.35	0.07
7160.54	13965.43	7158.58		W							
7157.44	13971.48	7155.48		W							
7141.46	14002.74	7139.51		W		20908.42	2	28047.91	1	7139.49	0.02
7129.08	14027.04	7127.13		W							
7100.92	14082.68	7098.98		W							
7086.25	14111.84	7084.31		W							
7075.26	14133.76	7073.33		W	B						
7066.08	14152.12	7064.15		W							
7060.24	14163.82	7058.31		W							
7046.81	14190.82	7044.88		W		48869.43	3	41824.58	3	7044.85	0.03
7012.60	14260.05	7010.68		W							

(1)	(2)	(3)	(4)	(5)	(6)	(7)	(8)	(9)	(10)	(11)	(12)
7000.16	14285.39	6998.25		W	AS	47702.41	2	40704.12	1	6998.29	-0.04
6977.90	14330.96	6975.99		W	AS						
6962.58	14362.49	6960.68		W							
6942.87	14403.27	6940.97		W							
6926.37	14437.58	6924.48		W	ASL						
6923.43	14443.71	6921.54		W							
6911.89	14467.82	6910.00	1	B	B						
6902.55	14487.40	6900.66	4	B							
6894.23	14504.88	6892.35	1	E							
6890.91	14505.56	6892.03	110	B							
6885.83	14522.58	6883.95	130	D		17901.28	5	24785.23	4	6883.95	0.00
6879.37	14536.21	6877.49	120	C							
6876.93	14541.37	6875.05	9	C							
6874.55	14546.41	6872.67	5	C		22880.24	3	29752.84	2	6872.60	0.07
6861.86	14573.31	6859.98	2	C							
6858.61	14580.21	6856.74	7	B							
6856.64	14584.40	6854.77	8	B		25678.60	3	32533.30	3	6854.70	0.07
6851.63	14595.07	6849.76	3	B							
6824.97	14652.08	6823.11	2	D							
6807.87	14688.88	6806.01	4	A							

(1)	(2)	(3)	(4)	(5)	(6)	(7)	(8)	(9)	(10)	(11)	(12)
6785.03	14738.33	6783.18	2	A							
6779.18	14751.05	6777.33	80	A		15673.33	3	22450.56	2	6777.23	0.10
6768.98	14773.27	6767.13	2	B		20784.87	1	14017.83	1	6767.04	0.09
6750.80	14813.06	6748.96	20	C		20784.87	1	27533.75	1	6748.88	0.08
6749.51	14815.89	6747.67	3	D							
6746.15	14823.27	6744.31	20	A							
6726.37	14866.86	6724.53	1	C							
6722.96	14874.40	6721.12	3	D							
6718.40	14884.50	6716.56	1	B	B						
6715.38	14891.19	6713.55	2	A							
6711.37	14900.09	6709.54	8	C							
6710.05	14903.02	6708.22	4	A							
6707.73	14908.17	6705.90	3	A							
6704.86	14914.55	6703.03	3	D							
6683.83	14961.48	6682.00	140	B		16766.60	4	23448.61	3	6682.01	-0.01
6671.20	14989.81	6669.38	20	B		40618.62	1	33949.28	3	6669.34	0.04
6669.26	14994.17	6667.44	1	A		39788.89	2	33121.48	2	6667.41	0.03
6667.40	14998.35	6665.58	1	B							
6663.44	15007.26	6661.62	6	A		45649.36	3	38987.83	4	6661.53	0.09
6662.18	15010.10	6660.36	2	D	B						

(1)	(2)	(3)	(4)	(5)	(6)	(7)	(8)	(9)	(10)	(11)	(12)
6659.44	15016.28	6657.62	2	C	B						
6655.47	15025.23	6653.65	7	D							
6650.23	15037.07	6648.41	10	E							
6641.45	15056.95	6639.64	3	D							
6637.00	15067.05	6635.19	1	B	B						
6628.56	15086.23	6626.75	1	C	B						
6582.72	15191.29	6580.92	1	B		36523.84	3	43104.71	3	6580.87	0.05
6534.03	15304.49	6532.25	1	B		48356.90	4	41824.58	3	6532.32	-0.07
6528.67	15317.06	6526.89	8	B							
6514.37	15350.68	6512.59	4	A							
6510.05	15360.87	6508.27	2	C	AS						
6495.17	15396.06	6493.40	2	B							
6480.85	15430.07	6479.08	3	D							
6475.31	15443.28	6473.54	7	B							
6473.99	15446.42	6472.22	1	C							
6465.16	15467.51	6463.39	2	C		30146.40	2	36609.85	3	6463.45	-0.06
6458.68	15483.04	6456.92	2	C							
6448.95	15506.40	6447.19	20	C							
6431.24	15549.10	6429.48	8	D	AS						
6427.21	15558.85	6425.45	20	D		31619.97	2	25194.47	1	6425.50	-0.05

(1)	(2)	(3)	(4)	(5)	(6)	(7)	(8)	(9)	(10)	(11)	(12)
6426.98	15559.40	6425.22	20	D		23327.71	2	29752.84	2	6425.13	0.09
6425.72	15562.46	6423.96	8	B							
6423.11	15568.78	6421.36	2	C		41298.36	2	34877.04	3	6421.32	0.04
6407.86	15605.83	6406.11	1	D		26715.37	3	33121.48	2	6406.11	0.00
6403.67	15616.05	6401.92	1	C							
6401.72	15620.80	6399.97	1	C							
6398.51	15628.64	6396.76	6	D							
6396.76	15632.91	6395.01	1	D	B						
6388.07	15654.18	6386.33	2	A							
6368.15	15703.15	6366.41	30	D	AS						
6366.45	15707.35	6364.74	9	B		25678.60	3	31943.31	4	6264.71	0.03
6365.95	15708.57	6364.21	1	B							
6341.15	15770.01	6339.42	2	B	AS						
6330.95	15795.42	6329.22	2	C							
6329.45	15799.16	6327.72	1	C	AS						
6312.51	15841.56	6310.79	2	C							
6292.13	15892.87	6290.41	2	B	B						
6289.14	15900.43	6287.42	1	C	B						
6285.22	15910.34	6283.50	3	A							
6264.24	15963.63	6262.53	1	C							

(1)	(2)	(3)	(4)	(5)	(6)	(7)	(8)	(9)	(10)	(11)	(12)
6262.16	15968.93	6260.45	1	C							
6260.12	15974.17	6258.41	2	B		25084.14	2	31342.51	3	6258.37	0.04
6243.09	16017.71	6241.38	4	C							
6238.07	16030.60	6236.37	3	D							
6235.86	16036.28	6234.16	1	D							
6224.07	16066.66	6222.37	1	C							
6221.68	16072.83	6219.98	1	C							
6216.99	16084.95	6215.29	1	A							
6204.10	16118.37	6202.41	2	B		34991.54	1	41193.97	1	6202.43	-0.02
6203.08	16121.00	6201.39	3	A		34991.54	1	28790.25	1	6201.29	0.10
6195.72	16140.17	6194.03	8	C							
6190.48	16153.84	6188.79	3	C							
6159.15	16236.01	6157.47	1	B							
6143.96	16276.15	6142.28	5	A							
6136.51	16296.91	6134.83	220	B	ASS	16766.60	4	22901.34	5	6134.74	0.09
6116.11	16350.26	6114.44	1	C	B	27074.50	4	20960.09	4	6114.41	0.03
6113.27	16357.86	6111.60	1	B							
6089.62	16421.39	6087.96	1	C	B						
6080.37	16446.37	6078.71	10	C		35115.28	2	41193.97	1	6078.69	0.02
6075.62	16459.23	6073.96	1	C							

(1)	(2)	(3)	(4)	(5)	(6)	(7)	(8)	(9)	(10)	(11)	(12)
6069.97	16474.55	6068.31	3	A							
6068.94	16477.34	6067.28	1	B							
6062.52	16494.79	6060.86	6	B		42670.81	4	36609.85	3	6060.96	-0.10
6060.54	16500.18	6058.88	3	A							
6012.32	16632.51	6010.68	3	A	AS	39788.89	2	45799.48	1	6010.59	0.09
6010.75	16636.86	6009.11	2	D		46966.61	3	40957.54	3	6009.07	0.04
5995.54	16679.06	5993.90	1	A	AS	23252.81	4	29246.65	4	5993.84	0.06
5990.85	16692.12	5989.21	1	A	B	25281.81	3	19292.69	3	5989.12	0.09
5989.09	16697.03	5987.45	3	A							
5986.41	16704.50	5984.78	7	A							
5980.10	16722.13	5978.47	4	A	AS						
5977.69	16728.87	5976.06	2	A							
5969.85	16750.84	5968.22	3	B		38289.38	2	44257.54	1	5968.16	0.06
5967.56	16757.27	5965.93	10	B		34991.54	1	40957.54	2	5966.00	-0.07
5933.69	16852.92	5932.07	1	D	AS	44777.50	4	38845.44	5	5932.06	0.01
5919.87	16892.26	5918.25	2	C							
5904.82	16935.32	5903.21	1	B		46860.72	2	40957.54	3	5903.18	0.03
5903.08	16940.31	5901.47	1	B							
5876.96	17015.60	5875.36	1	B							
5872.59	17028.26	5870.99	8	B	B						

(1)	(2)	(3)	(4)	(5)	(6)	(7)	(8)	(9)	(10)	(11)	(12)
5854.64	17080.47	5853.04	4	D	B						
5846.16	17105.25	5844.56	2	A		41298.36	2	35453.83	3	5844.53	0.03
5843.93	17111.77	5842.33	5	B		35115.28	2	40957.54	3	5842.26	0.07
5841.29	17119.51	5839.70	3	B	AS	39788.89	2	33949.28	3	5839.61	0.09
5831.82	17147.31	5830.23	2	B							
5826.86	17161.90	5825.27	1	C							
5825.20	17166.79	5823.61	1	D	AS						
5819.95	17182.28	5818.36	2	C	B						
5816.80	17191.58	5815.21	2	C	B						
5797.18	17249.77	5795.60	1	A							
5779.93	17301.25	5778.35	1	B		36523.84	3	42302.12		5778.28	0.07
5766.50	17341.54	5764.93	3	B							
5761.47	17356.68	5759.90	10	A							
5743.19	17411.93	5741.62	2	A							
5737.87	17428.07	5736.30	3	C							
5719.74	17483.31	5718.18	1	D	AS	31054.64	3	36772.85	2	5718.21	-0.03
5714.12	17500.51	5712.56	2	B		34991.54	1	40704.12	1	5712.58	-0.02
5705.03	17528.39	5703.47	70	A		22880.24	3	28583.69	3	5703.45	0.02
5700.61	17541.98	5699.05	10	A		14092.28	1	19791.30	2	5699.02	0.03
5695.73	17557.01	5694.17	2	B							

(1)	(2)	(3)	(4)	(5)	(6)	(7)	(8)	(9)	(10)	(11)	(12)
5684.30	17592.32	5682.75	2	C		41298.36	2	46981.20	2	5682.84	-0.09
5680.71	17603.43	5679.16	2	C		20784.87	1	26463.93	1	5679.06	0.10
5667.80	17643.53	5666.25	3	B		39788.89	2	45455.15	3	5666.26	-0.01
5658.06	17673.90	5656.52	1	B	AS	40513.55	2	46170.12	2	5656.57	-0.05
5655.24	17682.72	5653.70	1	B		31119.20	2	36772.85	2	5653.65	0.05
5653.78	17687.28	5652.24	9	A		35115.28	2	40767.44	3	5652.16	0.08
5638.05	17736.63	5636.51	1	A		40513.55	2	34877.04	3	5636.51	0.00
5631.87	17756.09	5630.33	1	A							
5630.31	17761	5628.77	1	E							
5629.31	17764.17	5627.77	1	C							
5628.07	17768.08	5626.53	1	C							
5624.40	17779.67	5622.86	1	C							
5620.61	17791.66	5619.08	1	B							
5611.20	17821.50	5609.67	1	A							
5601.38	17852.74	5599.85	2	B	AS						
5594.02	17876.23	5592.49	2	B							
5590.37	17887.90	5588.84	2	D		35115.28	2	40704.12	1	5588.84	0.00
5585.01	17905.07	5583.49	2	B							
5575.44	17935.80	5573.92	3	A							
5559.43	17987.46	5557.91	130	B		8983.75	2	14541.68	3	5557.93	-0.02

(1)	(2)	(3)	(4)	(5)	(6)	(7)	(8)	(9)	(10)	(11)	(12)
5556.33	17997.49	5554.81	1	E	AS						
5553.41	18006.95	5551.89		W							
5541.62	18045.26	5539.63		W							
5541.14	18046.83	5539.63		W	AS	46961.96	2	41422.43	3	5539.53	0.10
5533.25	18072.56	5531.74		W							
5499.47	18183.57	5497.97		W							
5484.37	18233.63	5482.87		W							
5479.00	18251.51	5477.50		W							
5464.02	18301.54	5462.53		W		23327.71	2	28790.25	1	5462.54	-0.01
5456.75	18325.93	5455.26		W		22199.08	3	27654.32	3	5455.24	-0.02
5453.50	18336.85	5452.01		W							
5452.88	18338.93	5451.39		W		8983.75	2	14435.13	2	5451.38	0.01
5421.88	18443.79	5420.40		W		31054.64	3	25634.21	2	5420.43	-0.03
5413.89	18471.01	5412.41		W							
5400.59	18516.50	5399.12		W							
5398.83	18522.53	5397.36		W		20908.42	2	26305.78	3	5397.36	0.00
5388.60	18557.70	5387.13		W		22880.24	3	28267.39	2	5387.15	-0.02
5372.69	18612.65	5371.22		W							
5358.31	18662.60	5356.85		W							
5351.45	18686.52	5349.99		W							

(1)	(2)	(3)	(4)	(5)	(6)	(7)	(8)	(9)	(10)	(11)	(12)
5341.54	18721.19	5340.08		W							
5332.31	18753.60	5330.85		W		23253.81	4	28583.69	3	5330.88	-0.03
5318.88	18800.95	5317.43		W		22199.08	3	27516.41	4	5317.33	0.10
5318.11	18803.67	5316.66		W		23327.71	2	18011.05	2	5316.66	0.00
5302.16	18860.24	5300.71		W		36523.84	3	41824.58	3	5300.74	-0.03
5297.48	18876.90	5296.03		W							
5296.77	18879.43	5295.32		W							
5288.28	18909.74	5286.84		W		15673.33	3	20960.09	4	5286.76	0.08
5281.03	18935.70	5279.59		W	AS						
5266.85	18986.68	5265.41		W	B						
5264.59	18994.83	5263.15		W							
5257.42	19020.74	5255.98		W		23327.71	2	28583.69	3	5255.98	0.00
5255.77	19026.71	5254.34		W							
5237.37	19093.55	5235.94		W	AS						
5229.68	19121.63	5228.25		W							
5229.26	19123.16	5227.83		W							
5228.53	19125.83	5227.10		W		45994.60	3	40767.44	3	5227.16	-0.06
5219.55	19158.70	5218.14		W							
5219.27	19159.77	5217.85		W							
5215.35	19174.17	5213.93		W							

(1)	(2)	(3)	(4)	(5)	(6)	(7)	(8)	(9)	(10)	(11)	(12)
5174.47	19325.65	5173.06		W							
5162.88	19369.03	5161.47	30	B		24085.14	5	29246.65	4	5161.51	-0.04
5160.89	19376.50	5159.48	1	C							
5150.44	19415.82	5149.03	2	A	B						
5147.72	19426	5146.32	1	E							
5145.62	19434	5144.22	2	E							
5144.20	19439.37	5142.80	1	C							
5140.60	19452.98	5139.20	2	E							
5139.38	19457.60	5137.98	1	C		30146.40	2	35384.33	1	5137.93	0.05
5120.41	19529.69	5119.01	1	A							
5119.91	19531.59	5118.51	1	A		35115.28	2	29996.81	3	5118.47	-0.04
5113.28	19556.92	5111.88	5	A							
5055.99	19778.52	5054.61	3	A		25678.60	3	30733.22	4	5054.62	-0.01
5052.05	19793.95	5050.67	20	A		14740.68	2	19791.30	2	5050.62	0.05
5038.28	19848.04	5036.90	1	A							
5035.50	19859.00	5034.13	6	A		26918.14	1	31952.25	1	5034.11	0.02
5029.29	19883.52	5027.92	6	B		23252.81	4	18224.99	4	5027.82	0.10
5013.28	19947.02	5011.91	1	A	AS						
5005.93	19976.31	5004.56	1	B	B						
5001.42	19994.32	5000.06	1	A		17901.28	5	22901.34	5	5000.06	0.00

(1)	(2)	(3)	(4)	(5)	(6)	(7)	(8)	(9)	(10)	(11)	(12)
4998.54	20005.84	4997.18	1	D							
4967.19	20132.11	4965.83	2	B		37336.20	1	42302.12	2	4965.92	-0.09
4943.47	20228.71	4942.12	10	B	AS						
4922.86	20313.40	4921.52	1	C	AS						
4916.93	20337.89	4915.59	6	A							
4914.00	20350.02	4912.66	20	C							
4899.98	20408.25	4898.64	2	B		36523.84	3	41422.43	3	4898.59	0.05
4898.12	20416	4896.78	1	E							
4896.84	20421.33	4895.50	1	C		26715.37	3	31610.80	2	4895.43	0.07
4888.92	20454.42	4887.59	6	C	AS						
4886.19	20465.84	4884.86	1	C							
4871.65	20526.93	4870.32	170	A							
4870.51	20531.72	4869.18	2	A		22880.24	3	18011.05	2	4869.19	-0.01
4869.59	20535.61	4868.26	20	C							
4850.69	20615.62	4849.37	30	B		20784.87	1	25634.21	2	4849.34	-0.03
4844.96	20640	4843.64	2	E							
4797.77	20843	4796.46	2	E							
4775.41	20940.61	4774.11	50	B		22880.24	3	27654.32	3	4774.08	0.03
4746.39	21068.64	4745.09	2	A	AS	20908.42	2	16163.36	2	4745.06	0.03
4731.15	21136.51	4729.86	3	A							

(1)	(2)	(3)	(4)	(5)	(6)	(7)	(8)	(9)	(10)	(11)	(12)
4727.06	21154.80	4725.77	40	A		20908.42	2	25634.21	2	4725.79	-0.02
4716.26	21203.24	4714.97	4	B		25281.81	3	29996.81	3	4715.00	-0.03
4715.20	21208	4713.91	1	E							
4710.09	21231	4708.80	2	E							
4670.02	21413.18	4668.75	1	B		25084.14	2	29752.84	2	4668.70	0.05
4663.31	21444	4662.04	1	E							
4657.24	21471.94	4655.97	1	C	AS						
4656.59	21474.94	4655.32	2	D		22880.24	3	18224.99	4	4655.25	0.07
4652.86	21492.16	4651.59	1	C							
4637.49	21563.39	4636.22	1	B		22880.24	3	27516.41	4	4636.17	0.05
4627.25	21611.11	4625.99	8	A							
4622.77	21632.05	4621.51	2	B		20784.87	1	16163.36	2	4621.51	0.00
4618.55	21651.82	4617.29	1	C	B	31619.97	2	36237.34	3	4617.37	-0.08
4615.62	21665.56	4614.36	1	A							
4611.44	21685.20	4610.18	2	B							
4610.63	21689	4609.37	1	E							
4590.39	21784.64	4589.14	3	A		35115.28	2	39704.41	1	4589.13	0.01
4575.42	21855.92	4574.17	1	C							
4553.25	21962.33	4552.01	140	A		14740.68	2	19292.69	3	4552.01	0.00
4502.07	22212	4500.84	1	E							

(1)	(2)	(3)	(4)	(5)	(6)	(7)	(8)	(9)	(10)	(11)	(12)
4500.86	22217.98	4499.63	1	E							
4500.54	22219.55	4499.31	1	D							
4481.29	22315	4480.07	1	E							
4473.47	22354	4472.25	1	E							
4472.39	22359.41	4471.17	1	C							
4472.07	22361	4470.85	2	E							
4439.37	22525.72	4438.16	2	C		41211.03	2	36772.85	2	4438.18	-0.02
4419.28	22628.12	4418.07	1	C							
4412.94	22660.63	4411.74	1	D							
4410.90	22671.11	4409.70	30	B		20784.87	1	25194.47	1	4409.60	0.10
4407.84	22686.85	4406.64	1	B							
4402.75	22713.08	4401.55	8	B		23252.81	4	27654.32	3	4401.51	0.04
4377.18	22845.76	4375.99	2	C							
4338.12	23051.46	4336.94	1	C	B						
4335.80	23063.79	4334.62	3	A		31119.20	2	35453.83	3	4334.63	-0.01
4327.82	23106.32	4326.64	7	B		23327.71	2	27654.32	3	4326.61	0.03
4322.98	23132.19	4321.80	1	C		25281.81	3	20960.09	4	4321.72	0.08
4321.05	23142.52	4319.87	1	B	AS	35115.28	2	39435.20	2	4319.92	-0.05
4320.96	23143	4319.78	2	E							
4319.43	23151.20	4318.25	2	B							

(1)	(2)	(3)	(4)	(5)	(6)	(7)	(8)	(9)	(10)	(11)	(12)
4318.16	23158	4316.98	1	E							
4313.52	23182.92	4312.34	2	B							
4287.24	23325.03	4286.07	10	A		20908.42	2	25194.47	1	4286.05	0.02
4269.09	23424.20	4267.93	1	C		27074.50	4	31342.51	3	4268.01	-0.08
4232.90	23624.47	4231.75	4	C		39286.19	1	43517.85	2	4231.66	0.09
4207.16	23769.00	4206.01	2	B		41475.84	3	37169.82	4	4206.02	-0.01
4183.12	23905.60	4181.98	10	B		20784.87	1	24966.78	0	4181.91	0.07
4122.18	24259	4121.06	1	E							
4120.75	24267.43	4119.63	1	C		25281.81	3	29401.44	2	4119.63	0.00
4119.07	24277.32	4117.95	2	B	B	15673.33	3	19791.30	2	4117.97	-0.02
4118.54	24280.45	4117.42	1	A							
4107.83	24343.75	4106.71	6	B		22199.08	3	26305.78	3	4106.70	0.01
4084.45	24483.10	4083.34	1	C							
4052.19	24678.01	4051.08	6	C		14092.28	1	18143.37	1	4051.09	-0.01
4043.71	24729.77	4042.61	1	B							
4034.14	24788.43	4033.04	2	A							
4018.92	24882.31	4017.82	2	A		26715.37	3	30733.22	4	4017.85	-0.03
4010.38	24935.29	4009.29	200	B	ASL						
3981.37	25116.98	3980.28	1	E	B						
3975.18	25156.09	3974.10	2	B		22199.08	3	18224.99	4	3974.09	0.01
3961.20	25244.88	3960.12	4	C		23252.81	4	19292.69	3	3960.12	0.00

CHAPTER 5

CONCLUSIONS

In the present analysis of the hafnium spectrum wavenumbers of 521 lines of Hf I in the wavelength range 1.0 - 2.5 μm have been measured with an average accuracy of 0.05 cm^{-1}. The intensities of 457 lines, lying outside the strong water vapour absorption regions (1.3 - 1.45 μm and 1.8 - 1.95 μm) have been measured with an average accuracy of 10% and have been put on a uniform scale. About 220 observed lines have been assigned to the known energy levels of Hf I;.The largest difference between the observed and the calculated wave numbers was 0.1 cm^{-1}. It was not possible to confirm the line assignments and there were probably some accidental coincidences. The intensities of the lines assigned to levels of known term classification conform to the intensity rules of multiplet transitions and the "experimental line strengths" agree with the theoretical line strengths.

The positions of the levels of the even configurations $5d^4$, $5d^36s$ and $5d^26s^2$ of Hf I have been calculated assuming intermediate coupling. The calculation of levels of the ground configuration was unsatisfactory and the differences between the observed and the calculated values of the energy levels of this configuration were large. The Coulomb interaction parameters F^2 and F^4 were not "well behaved"; F^4 being greater than F^2 in some cases. The physically unrealistic values of the Coulomb interaction parameters and the large differences between the observed and the calculated positions of the energy levels of configuration $5d^26s^2$ were probably caused either by wrong levels being assigned to this configuration or by the perturbation of the levels of this configuration by levels which have not yet been discovered. The perturbation appeared to be largest for levels with total angular momentum quantum number of two and the agreement which the level separations

have with the Lande interval rule is probably fictitious. It has not been possible to determine the physical reasons for the large differences between the observed and the calculated positions of the configurations $5d^26s^2$, although an empirical relation is determined which gave a better agreement between the observed and the calculated wavenumbers of the energy levels.

The positions of the levels of the configuration $5d^36s$ have been calculated using the known energy levels of this configuration to improve the interaction parameters by the method of least squares. The Coulomb interaction parameters in this case were well behaved and the root mean square error between the observed and the calculated positions of the energy levels was 1% of the configuration width. The results of this calculation were used to assign new levels to the configuration $5d^36s$. Seven more levels have been assigned to this configuration but the root mean square error has increased to 2% of the configuration width. The new and the old levels have been used to obtain better estimates of the interaction parameters of this configuration. The Coulomb, the exchange, and the spin-orbit interaction parameters obtained during the calculation of the positions of the levels of the configuration $5d^36s$ have been used to obtain approximate positions of the levels of the configuration $5d^4$ but it has not been possible to assign any of the observed levels to this configuration.

The theoretical calculations of the energy levels of the low even configurations of Hf I ($5d^26s^2$, $5d^36s$ and $5d^4$) can be improved by including the configuration interaction between these three configurations in the calculations of the energy matrices. The calculation of the exact value of the interaction parameters would be greatly assisted by assigning more levels to these configurations and by locating the unknown levels.

The experimental procedure to obtain the infrared spectrum of Hf I can be improved considerably. The method used to sublime hafnium iodide was quite unsatisfactory and could have resulted in impurities appearing in the discharge tube. A thermostatically controlled furnace maintained at 400°C (sublimation temperature of hafnium iodide) would have been a more certain way of ensuring that only hafnium iodide was sublimed into the discharge tube.

The inaccuracies in the wavenumbers were caused by the spectrum being scanned unevenly across the exit slit. The screw and the nut used to rotate the grating in the spectrometer used during the present project need to be replaced. A merton nut and a new set of bearings to hold the screw in place would have improved the smoothness of the scan resulting in an improved accuracy of the wavenumbers. The accuracy of the wavenumbers could also have been increased by more closely spaced fringes. A wider spacer (1.5 mm) for the Febry-Perot etalon to record fringes every 0.5 cms of the chart would probably have reduced the average inaccuracy of the wavenumbers by a factor of two. The Edser-Butler fringe method of calibrating a spectrometer has some disadvantages; the main disadvantage being the limited length of slit available for the spectral beam. This disadvantage could have been overcome by using longer slits for the spectrometer as with curved slits astigmatism would not have been a problem. The ideal refinement would have been two independently adjustable pairs of slits, one for the spectral beam and another for the calibration beam. The problem of insufficient slit length for the spectral and the calibration beams can also be resolved by electronically separating the output signals due to the two light beams. The 'AND' gates developed during the present project could separate different sections of a waveform but were useless without an amplifier which produced little or no distortion at low frequencies.

The intensities of hafnium lines need to be measured with far greater accuracy than has been possible during the present analysis of hafnium spectrum, although the present measurements have proved quite useful in spectral line classification. The most serious source of error in the intensity measurements was probably the uncertainty in the true background level and it may not be possible to eliminate this source of error completely. The present intensity values could be improved by multiple measurements and by using a phase sensitive amplifier to increase the signal to noise ratio although in this case rather slow scanning speeds may be necessary. The accurate estimate of intensities would be necessary to determine if the population of the energy levels could be described in terms of an excitation temperature. It may be necessary to determine the existence and the magnitude of excitation temperature in various parts of the discharge to see if local thermodynamic equilibrium conditions hold in a microwave excited hafnium discharge. Preliminary results from experiments with microwave excited neon discharge seemed to indicate that the discharge could be described in terms of an excitation temperature but in this work neon lines with closely spaced upper energy levels were studied. Similar work on microwave excited hafnium discharges would have enabled corrections to be made for the self-absorption of the emitted spectral lines. It seems strange that in view of the extreme stability and sharpness of the spectral lines emitted by microwave excited discharges, that these sources should have been completely ignored as far as intensity and oscillator strength measurements of spectral lines are concerned.

Finally, the theoretical analysis of the even configurations should be extended to other possible even configurations, viz $5d^26p^2$, $5d^26s6d$, to determine the levels which could perturb the ground configuration. Similar calculations need to be carried out to determine the levels of the odd

configurations of Hf I, particularly the levels of the configuration $5d^3 6p$ as most of the levels of the lowest odd configuration $5d^2 6s 6p$ are known.

APPENDIX 1

SPIN-ORBIT INTERACTION MATRICES OF CONFIGURATIONS d^3s and d^4

The coefficient matrices for spin-orbit interaction within the configurations d^3s were calculated from[50,51],

$$(d^3(vSL)sS_1LJ \mid \underline{l}_1 \cdot \underline{s}_1 \mid d^3(v^1S^1L^1)sS_1^1L^1J)$$
$$= (-)^{L^1-S^1-\frac{1}{2}-J}(30)^{\frac{1}{2}}(d^3vSL \parallel V^{11} \parallel d^3v^1S^1L^1)$$
$$\times \left[(2S_1+1)(2S_1^1+1)\right]^{\frac{1}{2}} W(SS_1^1LL^1;IJ)W(SS_1S^1S_1^1;\tfrac{1}{2}1) \qquad \text{A.1.1.}$$

where v and v^1 are the seniority numbers of the multiplets of the configuration d^3

S and S^1 are the total spin angular momentum quantum numbers of multiplet of d^3

S_1 and S_1^1 are the total spin angular momentum quantum numbers of the multiplet of d^3s

L and L^1 are the total orbital angular momentum quantum numbers of the multiplets of d^3

J is the total angular momentum quantum number of the levels of d^3s.

The matrices are given in Table A.1.1.

The coefficient matrices for spin-orbit interaction within the configuration d^4 were calculated from[43,47]

$$(d^4vSLJ \mid \underline{l}_1 \cdot \underline{s}_1 \mid d^4v^1S^1L^1J)$$
$$= (-)^{S+L^1-J}(30)^{\frac{1}{2}}(d^4vSL \parallel V^{11} \parallel d^4v^1S^1L^1)W(SS^1LL^1;1J) \qquad \text{A.1.2.}$$

where v and v^1 are the siniority numbers

S and S^1 are the total spin-angular momentum quantum number

L and L^1 are the total orbital angular momentum quantum number

J is the total angular momentum quantum number.

The matrices are given in Table A.1.2.

In the relations A.1.1. and A.1.2. the reduced matrix elements,

$(d^n \ldots\ldots \| V^{11} \| d^n \ldots\ldots)$, were obtained from tables given by Slater (1960)[43]. The Racah functions, W (abcd;ef), were calculated for each case.

TABLE A 1.1.

SPIN-ORBIT MATRICES FOR THE CONFIGURATION d^3s

J=6

^3H
$\frac{1(1)^{1/2}}{2}$

J=5

^5F	^3H	^3G	^1H
$\frac{3(70)^{1/2}}{4}$	0	$\frac{1(105)^{1/2}}{2}$	0
	$\frac{-1(1)^{1/2}}{30}$	$\frac{-6(1)^{1/2}}{5}$	$\frac{-1(30)^{1/2}}{10}$
		$\frac{3(1)^{1/2}}{5}$	$\frac{-1(30)^{1/2}}{5}$
			0

J=4

^5F	^3H	^3G	$^3F_1$	$^3F_2$	^1G
$\frac{1(105)^{1/2}}{20}$	0	$\frac{1(30)^{1/2}}{24}$	$\frac{-1(5)^{1/2}}{4}$	$\frac{1(2)^{1/2}}{8}$	0
	$\frac{-3(1)^{1/2}}{5}$	$\frac{-2(66)^{1/2}}{3}$	0	0	$\frac{1(330)^{1/2}}{15}$
		$\frac{-3(1)^{1/2}}{20}$	$\frac{-5(3)^{1/2}}{12}$	$\frac{5(3)^{1/2}}{12}$	$\frac{-3(5)^{1/2}}{10}$
			$\frac{5(1)^{1/2}}{4}$	$\frac{-1(1)^{1/2}}{4}$	$\frac{1(60)^{1/2}}{6}$
				$\frac{-1(1)^{1/2}}{4}$	$\frac{1(60)^{1/2}}{12}$
					0

TABLE A11.1.(cont.)

^5F ^5P ^3G $^3F_1$ $^3F_2$ $^3D_1$ $^3D_2$ ^1F

$J=3$

^5F	^5P	^3G	$^3F_1$	$^3F_2$	$^3D_1$	$^3D_2$	^1F
$-3(1)^{1/2}/4$	0	$5(7)^{1/2}/28$	$-1(5)^{1/2}/4$	$-1(5)^{1/2}/4$	$1(15)^{1/2}/1$	$-1(35)^{1/2}/7$	0
	$-1(1)^{1/2}/2$	0	0	0	$2(15)^{1/2}/5$	0	0
		$-3(1)^{1/2}/4$	$-1(15)^{1/2}/2$	$1(15)^{1/2}/2$	0	0	$1(105)^{1/2}/14$
			$5(2)^{1/2}/24$	$1(2)^{1/2}/24$	$-1(3)^{1/2}/3$	$5(63)^{1/2}/63$	$1(3)^{1/2}/3$
				$1(1)^{1/2}/12$	$-2(3)^{1/2}/3$	$-2(63)^{1/2}/63$	$1(3)^{1/2}/6$
					$-1(1)^{1/2}/2$	$-1(21)^{1/2}/6$	$-1(1)^{1/2}/1$
						$1(1)^{1/2}/6$	$-1(21)^{1/2}/21$
							0

TABLE A 1.1.(cont.)

J=2

^5F	^5P	$^3F_1$	$^3F_2$	$^3D_1$	$^3D_2$	$^3P_1$	$^3P_2$	$^1D_1$	$^1D_2$
$-3(1)^{1/2}/2$	0	$-1(6)^{1/2}/6$	$-1(6)^{1/2}/6$	$1(35)^{1/2}/5$	$-(15)^{1/2}/3$	0	0	0	0
	$5(5)^{1/2}/36$	0	0	$1(15)^{1/2}/5$	0	$-1(1)^{1/2}/4$	$-1(14)^{1/2}/2$	0	0
		$-5(1)^{1/2}/3$	$1(10)^{1/2}/6$	$1(210)^{1/2}/30$	$-1(10)^{1/2}/6$		0	$1(35)^{1/2}/5$	$-1(15)^{1/2}/3$
			$1(1)^{1/2}/3$	$-1(210)^{1/2}/15$	$-1(10)^{1/2}/15$	0	0	$2(10)^{1/2}/5$	$2(210)^{1/2}/105$
				$-1(1)^{1/2}/4$	$1(21)^{1/2}/12$	$-1(15)^{1/2}/5$	$1(210)^{1/2}/20$	$-1(6)^{1/2}/4$	$1(14)^{1/2}/4$
					$1(21)^{1/2}/12$	0	$-9(10)^{1/2}/20$	$1(14)^{1/2}/4$	$1(6)^{1/2}/12$
						$5(1)^{1/2}/12$	$-1(14)^{1/2}/6$	$2(10)^{1/2}/5$	0
							$-1(10)^{1/2}/12$	$1(35)^{1/2}/10$	$-3(15)^{1/2}/10$
								0	$1(21)^{1/2}/12$
									0

TABLE A 1.1 .(cont.)

J=1

^5P	^5P	$^3D_1$	$^3D_2$	$^3P_1$	$^3P_2$	^1P
$-2(1)^{1/2}/1$	0	$1(210)^{1/2}/10$	$-1(10)^{1/2}/2$	0	0	0
	$-3(1)^{1/2}/4$	$1(15)^{1/2}/15$	0	$1(5)^{1/2}/12$	$1(70)^{1/2}/6$	0
		$-3(1)^{1/2}/4$	$1(105)^{1/2}/12$	$1(3)^{1/2}/3$	$1(42)^{1/2}/12$	$-1(21)^{1/2}/6$
			$1(1)^{1/2}/4$	0	$3(2)^{1/2}/4$	$3(1)^{1/2}/2$
				$-5(1)^{1/2}/12$	$-1(14)^{1/2}/6$	$-2(7)^{1/2}/3$
					$-1(1)^{1/2}/3$	$-2(7)^{1/2}/3$
						0

J=0

$^3\Pi$	$^3\Pi_2$
$5(1)^{1/2}/6$	$1(14)^{1/2}/6$
	$-2(1)^{1/2}/3$

TABLE A 1.2.

SPIN-ORBIT MARTICES FOR THE CONFIGURATION d^4

J=6

^3H	^1I
$\frac{1(1)^{1/2}}{2}$	$\frac{1(6)^{1/2}}{2}$
0	

J=5

^3G	^3H
$\frac{3(1)^{1/2}}{5}$	$\frac{-6(1)^{1/2}}{5}$
	$\frac{-1(1)^{1/2}}{10}$

J=4

^5D	$^3F_1$	$^3F_2$	$^1G_1$	$^1G_2$	^3G	^3H
$\frac{1(1)^{1/2}}{1}$	$\frac{1(2)^{1/2}}{1}$	$\frac{-1(2)^{1/2}}{1}$	0	0	0	0
	$\frac{1(1)^{1/2}}{2}$	$\frac{-1(1)^{1/2}}{2}$	$\frac{1(1)^{1/2}}{3}$	$\frac{-1(11)^{1/2}}{3}$	$\frac{-5(3)^{1/2}}{6}$	0
		$\frac{-1(1)^{1/2}}{4}$	$\frac{-5(1)^{1/2}}{3}$	$\frac{1(11)^{1/2}}{6}$	$\frac{5(3)^{1/2}}{12}$	0
			0	0	$\frac{1(3)^{1/2}}{3}$	$\frac{1(22)^{1/2}}{3}$
				0	$\frac{1(33)^{1/2}}{6}$	$\frac{-2(2)^{1/2}}{3}$
					$\frac{-3(1)^{1/2}}{20}$	$\frac{-2(66)^{1/2}}{15}$
						$\frac{-3(1)^{1/2}}{5}$

TABLE A 1.2.(cont.)

J=3

^3D	^5D	^1F	$^3F_1$	$^3F_2$	^3G
$\frac{1(1)^{1/2}}{6}$	$\frac{1(42)^{1/2}}{6}$	$\frac{2(105)^{1/2}}{21}$	$\frac{-10(7)^{1/2}}{21}$	$\frac{-2(7)^{1/2}}{21}$	0
	0	0	$\frac{1(6)^{1/2}}{3}$	$\frac{-1(6)^{1/2}}{3}$	0
		0	$\frac{1(15)^{1/2}}{3}$	$\frac{1(15)^{1/2}}{6}$	$\frac{3(21)^{1/2}}{14}$
			$\frac{-1(1)^{1/2}}{6}$	$\frac{1(1)^{1/2}}{6}$	$\frac{-3(15)^{1/2}}{14}$
				$\frac{1(1)^{1/2}}{12}$	$\frac{3(15)^{1/2}}{28}$
					$\frac{-3(1)^{1/2}}{4}$

J=2

^3P	^3P	$^1D_1$	$^1D_2$	$^3D_1$	$^5D_2$	$^3F_1$	$^3F_2$
$\frac{1(1)^{1/2}}{6}$	$\frac{-1(14)^{1/2}}{3}$	$\frac{1(210)^{1/2}}{30}$	$\frac{-2(105)^{1/2}}{15}$	0	$\frac{2(105)^{1/2}}{15}$	0	0
	$\frac{1(1)^{1/2}}{3}$	$\frac{-2(15)^{1/2}}{15}$	$\frac{-1(30)^{1/2}}{30}$	$\frac{-9(10)^{1/2}}{20}$	$\frac{-7(30)^{1/2}}{60}$	0	0
		0	0	$\frac{2(6)^{1/2}}{3}$	0	$\frac{-2(15)^{1/2}}{15}$	$\frac{-4(15)^{1/2}}{15}$
			0	$\frac{-1(3)^{1/2}}{3}$	0	$\frac{-1(30)^{1/2}}{15}$	$\frac{4(30)^{1/2}}{15}$
				$\frac{1(1)^{1/2}}{12}$	$\frac{7(3)^{1/2}}{12}$	$\frac{-1(10)^{1/2}}{3}$	$\frac{-1(10)^{1/2}}{15}$
					$\frac{-3(1)^{1/2}}{4}$	$\frac{1(30)^{1/2}}{15}$	$\frac{-1(30)^{1/2}}{15}$
						$\frac{-2(1)^{1/2}}{3}$	$\frac{2(1)^{1/2}}{3}$
							$\frac{1(1)^{1/2}}{3}$

TABLE A 1.2.(cont.)

J=1

$^1P_1$	$^3P_2$	^3D	^5D
$\frac{-1(1)^{1/2}}{6}$	$\frac{1(14)^{1/2}}{3}$	0	$\frac{2(1)^{1/2}}{1}$
	$\frac{-1(1)^{1/2}}{3}$	$\frac{-3(2)^{1/2}}{4}$	$\frac{-1(14)^{1/2}}{4}$
		$\frac{1(1)^{1/2}}{4}$	$\frac{1(7)^{1/2}}{4}$
			$\frac{-5(1)^{1/2}}{4}$

J=0

$^1S_1$	$^1S_2$	$^3P_1$	$^3P_2$	^5D
0	0	$\frac{-3(1)^{1/2}}{1}$	0	0
	0	$\frac{1(21)^{1/2}}{3}$	$\frac{-2(6)^{1/2}}{3}$	0
		$\frac{-1(1)^{1/2}}{3}$	$\frac{2(14)^{1/2}}{3}$	$\frac{4(3)^{1/2}}{3}$
			$\frac{-2(1)^{1/2}}{3}$	$\frac{-1(42)^{1/2}}{6}$
				$\frac{-3(1)^{1/2}}{2}$

APPENDIX 2

COMPUTER PROGRAMS DEVELOPED DURING THE ANALYSIS OF INFRARED SPECTRUM OF Hf I

Three main computer programs were designed during the analysis of infrared spectrum of Hf I. The three programs, described below, are:

1. A program to assign the infrared hafnium lines to the known energy levels of Hf.
2. A routine to diagonalise real symmetric matrices.
3. A routine to calculate, by least squares, the interaction parameters; by comparing the eigenvalues of the energy matrices with the known energy levels of Hf I.

LEVEL ASSIGNING PROGRAM:

The input data were, the observed air-wavenumbers, and the even and the odd energy levels with their respective total angular momentum quantum numbers - J. The program, written in Algol, comprised three steps. First, the input air wavenumbers were converted to vacuum wavenumbers by Edlens formula[33]. Second, a wavenumber of a theoretical line, in the range 3000-10000 cm^{-1}, was calculated by differencing a pair of even and odd energy levels which satisfied the selection rule $J = 0, \pm 1$ with $J = 0$ $J = 0$ forbidden. Third, the calculated wavenumber was compared with all the observed wavenumbers. If the wavenumbers agreed within a given accuracy, the observed wavenumber and the possible transition levels were printed. This procedure was repeated for all possible theoretical wavenumbers. The program is given below.

```
"BEGIN"
"REAL" "ARRAY" EE, EO [1 : 1 60],SIG1, SIG2 [1 : 500],INT[0:5];
"INTEGER" "ARRAY" PO, JO,PE,JE[1 : 1 60];
"INTEGER" C1,C2,C3,I,J,K,N;
"REAL" S,DIFF,C;
"PRINT" "L'P07P42',
 "L'TRANSITION LEVELS OF THE OBSERVED LINES', "L3", "R100";
C1:=C2=C3=N:=0;
L1:C1=C1+1; "READ" PE[C1],JE[C1],EE[C1];
"IF" PE[C1]"GE" 0 "THEN" "GO TO" L1;
L2:C2:=C2+1; "READ" PO[C2],JO[C2],EO[C2];
"IF" PO[C2] "GE" 0 "THEN" "GO TO" L2;
L3:C3:=C3+1; "READ" SIG1 [C3];
"IF" SIG1[C3] > 1.0 "THEN" "GO TO" L3;
C1:=C1-1;
C2:=C2-1;
C3:=C3-1;
"FOR" I:=1 "STEP" 1 "UNTIL" C3 "DO" "BEGIN"
INT[0]:=SIG1[I];
"FOR" N:=1 "STEP" 1 "UNTIL" 5 "DO" "BEGIN"
INT[N]:=INT[0]/(1+(6432.8_10 -8)+(294981000/((146.0_10 +8)-(INT[N-1] 2)))+
(25540.0/((41.0_10 +8)-(INT[N-1] 2))));
"IF" INT[N-1]-INT[N]<0.001 "THEN" "BEGIN"
SIG1[I]:=INT[N]; "GO TO"L8; "END"; END; L8:"END";
N:=0;
"FOR" I:=1 "STEP" 1 "UNTIL" C1 "DO" "BEGIN"
"FOR" J:=1 "STEP" 1 "UNTIL" C2 "DO" "BEGIN"
S:=ABS(EE[I]-EO[J]);
"IF" S "GE" 3300.0 "THEN" "BEGIN"
"IF" S "LE" 110000.0 "THEN" "BEGIN"
"IF" JE[I]=JO[J] "THEN" "GO TO" L4;
"IF" JE[I]=JO[J]-1 "THEN" "GO TO" L5;
"IF" JE[I]=JO[J]+1 "THEN" "GO TO" L5;
```

/Contd:

```
L4:"IF" JE[I]=Ø "THEN" "GO TO" L6;
L5:"FOR" K:=1 "STEP" 1 "UNTIL" C3 "DO" "BEGIN"
DIFF:=(S-SIG1[K]);
"IF" ABS( DIFF) "LE" Ø.1 "THEN" "BEGIN"
N:=N+1;
SIG2[N]:=SIG1[K];
"PRINT* ALIGNED(5,2),(SIG2[N])*
(1+(6432.8₁₀ -8)+(294981Ø.Ø/((146.Ø₁₀ +8)-(SIG2[N]↑ 2)))+
(2554Ø.Ø/((41.Ø₁₀ +8)-(SIG2[N]↑2)))),
SAMELINE,"S1",ALIGNED(5,2),SIG2[N],"S2",DIGITS(1),PE[I],
"S1",DIGITS(1),JE[I],"S1",ALIGNED(5,2),EE[I],"S2",
DIGITS(1),PO[J], DIGITS(1),JO[J], ALIGNED(5,2),EO[J],"S2",
ALIGNED(5,2),S,"S2"ALIGNED(1,3),DIFF;
"GO TO" L6;
"END"; "END"; "END"; "END"; L6:"END"; "END";
"END";
```

ROUTINE FOR DIAGONALISING REAL SYMMETRIC MATRICES

The method of diagonalising real symmetric matrices was invented by C.G.J. Jacobi and has been treated quite extensively in the literature. The aim of the method is to obtain an orthogonal matrix S which can transform a real symmetric matrix A into a diagonal matrix D. The ith. diagonal element of D can then be adopted as the ith. eigenvalue of A. The method[54,55] consists of annihilating in turn, the selected off-diagonal elements (pivotal elements) of A by orthogonal transformation. Each transformation affects many more elements than just those in the pivotal set, and in general, a single pass through all the pivotal elements does not produce a diagonal matrix. Jacobi's method is thus an iterative method and has been shown by Jacobi to converge.

In the present method the orthogonal transformation was performed on a pivotal element if it exceeded a certain threshold value. The value of the threshold was reduced by a factor equal to the order of the matrix. This procedure was repeated till the magnitude of the off-diagonal elements was reduced below a given value. In the diagonalising routine, given below, W was the input energy matrix and was output as a diagonal matrix, the original matrix being destroyed. The eigen-functions were output as matrices and the magnitude of the off-diagonal element was reduced below the limit,

$$\frac{\text{RHO} \times \sqrt{(\text{SUM OF SQUARES OF OFF-DIAGONAL ELEMENTS})}}{\text{ORDER OF MATRIX.}}$$

where

$$\text{RHO} = 1.0 \times 10^{-10}$$

The square-root of the sum of squares of the off-diagonal elements of the energy matrix was used as a starting threshold value.

```
      SUBROUTINE DIGN (A,N,RHO)
      INTEGER P,Q
      REAL INT1, NORM1,NORM2,MU
      DIMENSION A(N,N)
      COMMON FP(10),S(10,10)
      EQUIVALENCE(TEMP,SINTCOST)
      DO 1 I=1,N
      DO 2 J=1,N
      S(I,J)=0
      S(I,1)=1.0
      NORM1=0
      DO 10 I=1,N
      DO 99 J=1,N
      RS=RS+A(I,J)*A(I,J)
   10 CONTINUE
      DS=DS+A(I,I)*A(I,I)
   99 CONTINUE
      RS=SQRT(RS-DS)
      IF(RS.GT.NORM1) NORM1=RS
      NORM=(RHO/N)*NORM1
      THR=NORM 1
      IND=0
      THR=THR/N
      DO 4 Q=2,N
      IZ=*-1
      DO 4 P=1,IZ
      IF (THR-ABS(A(P,Q))) 25,25, 4
      IND = 1
      V1 = A(P,P)
      V2 = A(P,Q)
      V3 = A(Q,Q)
      MU = 0.5 * (V1 - V3)
      IF (MU) 6,7,7
    6 SIGN = 1.0
      GO TO 8
    7 SIGN = -1.0
    8 OMEGA = SIGN*V2/SQRT(V2**2 + MU**2)
```

/Continued

```
      SINT = OMEGA/SQRT(2.0 *(1.0+SQRT(ABS(1.0-OMEGA**2))))
      COST = SQRT(ABS( 1.0 - SINT**2) )
      DO 13  I=1,N
      IF  ( I-Q) 15,14,15
15      IF (I-P) 16,14,16
16      INT1 = A(I,P)
      MU = A(I,Q)
      TEMP = INT1*SINT + MU*COST
      A(I,Q) = TEMP
      A(Q,I) = TEMP
      TEMP = INT1*COST - MU*SINT
      A(I,P) = TEMP
      A(P,I) = TEMP
14      CONTINUE
      IF (IVS-1)0  ,13,0
      INT1 = S(I,P)
      MU = S(I,Q)
      S(I,Q) = INT1*SINT + MU*COST
      S(I,P) = INT1*COST - MU*SINT
13      CONTINUE
      SINTCOST = SINT * COST
      COST2 = COST**2
      SINT2 = SINT**2
      A(P,P)=V1*COST2 +V3*SINT2 -2.0*V2*SINTCOST
      A(Q,Q) =V1*SINT2 +V3*COST2 +2.0*V2*SINTCOST
      TEMP = (V1-V3)*SINTCOST + V2*(COST2 - SINT2)
      A(P,Q)= TEMP
      A(Q,P)= TEMP
4     CONTINUE
      IF (IND) 20,20,21
21      IND=0
      GO TO 5
20      IF (NORM2 -THR) 3,22,22
22    CONTINUE
      RETURN
      END
```

ROUTINE FOR LEAST SQUARE ADJUSTMENT OF INTERACTION PARAMETERS:

In the central field approximation the elements of the energy matrices are given by (Eq. 4.3.) a relation of the form,

$$a_{ij} = \sum(r)\, C_{ij}^{r}\, p^{r} \qquad \text{A.2.1.}$$

where C_{ij}^{r} are the elements of the coefficient matrices and p^{r} are the interaction parameters. The energy matrices set up with the preliminary values of the interaction parameters have the eigenvalues E and the eigenvector X . The derivatives of the eigenvalues with respect to parameters are given by,(45,46)

$$\frac{\partial E_{\alpha}}{\partial p^{r}} = \sum(ij) x_{\alpha i} x_{\alpha j} C_{ij}^{r} \qquad \text{A.2.2.}$$

where x are the components of the eigenvectors. Since the eigenvalues of the Hamiltonian are first-order homogeneous functions of the parameters,

$$E_{\alpha} = \sum(r)\, \frac{\partial E_{\alpha}}{\partial p^{r}}\, p^{r} \qquad \text{A.2.3.}$$

from Euler's theorem.

Thus the eigenvalues can be approximated as functions of the parameters by the following linear formulae, which are accurate to first-order in the difference between final values of the parameters and their preliminary values,

$$E_{\alpha} = \sum(r)\sum(ij)\left[x_{\alpha i} x_{\alpha j} C_{ij}^{r}\right] p^{r} \qquad \text{A.2.4.}$$

$$= \sum(r)\, b_{\alpha r} p^{r} \qquad \text{A.2.5.}$$

The correct values of the energy levels can be calculated from Eq. A.2.5. if the correct parameters for all the possible interactions are used to evaluate the equations. It is, however, impossible to include all atomic interactions in calculating the energy matrices. It is also impossible to know the final values of the interaction parameters unless the correct wavefunctions are known. Eq. A.2.5. can however be used to improve the starting parameters used to diagonalise the energy matrices if the energy levels E_α are known. From Eq. A.2.5. it is possible to get m equations (for n parameters used to form the energy matrices) if there are m energy levels in the configurations used to set up the energy matrices. Usually m is greater than n (if less than n energy levels are known the method cannot be used). Eq. A.2.5. can be used to form a set of simultaneous equations for n unknown parameters, which can be solved by the method of least squares.

From Eq. A.2.5., the error in the αth level is[43]

$$\sum(r) b_{\alpha r} p^r - E_\alpha \qquad \text{A.2.6.}$$

the improved parameters are those which minimise the mean square error weighted by (2J + 1) (where J is the total orbital angular momentum quantum number J of the level). If the weight of a level is j_α it is necessary to minimise the quantity,

$$\sum(\alpha) j_\alpha \left[\sum(r) a_{\alpha r} p^r - E_\alpha\right]^2 \qquad \text{A.2.7.}$$

Differentiating quantity A.2.7. with respect to one of the parameters p^r (p^i say) and set the derivative equal to zero, it is possible to obtain the equation,

$$\sum(\alpha)\left[\sum(r) j_\alpha a_{\alpha r} a_{\alpha i}\right] p^r = \sum(\alpha) j_\alpha a_{\alpha i} E_\alpha \qquad \text{A.2.8.}$$

The routine given below sets up the n simultaneous equations from A.2.8. The simultaneous equations were solved for n parameters by the

Gaussian elimination method. The input to the routine consisted of the energy levels of the configurations with their statistical weights and the coefficients $a_{\alpha r}$ calculated from A.2.5. Levels which were not known or were doubtful and had to be excluded from calculations of improved parameters, were given weights of zero.

```
      SUBROUTINE LSF(A,B,J,N,M)
      DIMENSION A(M,N),B(M,N),R(M),J(M),P(10,10)
      COMMON FP(10),S(10,10)
      DO 2 I=1,10
      DO 1 K=1,10
      P(I,K)=0.0
    1 CONTINUE
      FP(I)=0.0
    2 CONTINUE
      DO 4 I=*,N
      DO 3 K=1,M
      P(I,1)=P(I,1)+J(K)*A(K,1)*B(K)
    3 CONTINUE
    4 CONTINUE
      DO 7 L=2,N+1
      DO 6 I=1,N
      DO 5 K=1,M
      P(I,L)=P(I,L)+J(K)*A(K,L-1)*A(K,I)
    5 CONTINUE
    6 CONTINUE
    7 CONTINUE
      DO 9 I=1,N
      DO 8 L=2,N+1
      P(I,L)=-P(I,L)
    8 CONTINUE
    9 CONTINUE
      IC,KC=N
      IN=1
   10 DO 12 I=IN,IC
      DO 11 K=1,KC
      P(I,K)=P(I,K)/P(I,KC+1)
   11 CONTINUE
   12 CONTINUE
      DO 14 I=IN+1,IC
      DO 13 K=1,KC
      P(I,K)=P(I,K)-P(IN,K)
   13 CONTINUE
```

/Continued

```
14  CONTINUE
    IN=IN+1
    KC=KC-1
    IF(IN-N) 10,0,0
    DO 15 I=1,N
    FP(I)=0.0
15  CONTINUE
    FP(1)=P(N,1)/P(N,2)
    DO 17 I=2,N
    DO 16 K=1,I-1
    FP(I)=FP(I)+P(N-1,K+1)*(-FP(K))
16  CONTINUE
    FP(I)=P(N-I+1)+FP(I)
17  CONTINUE
    DO 19 I=1,N
    FP(I)=-FP(I)
19  CONTINUE
    RETURN
    END
```

ACKNOWLEDGMENTS

The project described in this thesis was discussed with a number of people and the author is indebted to them for their advice and time spent on discussions. The author specially wishes to thank Dr. E.B.M.Steers of the Northern Polytechnic, London, for his frequent and useful comments at all stages of this project. The author would also like to thank Dr. J.W.King for his literary comments on the draft of the first chapter of this thesis. The author is grateful to Mrs. P.L.Elvins, for typing a somewhat difficult manuscript. Finally, the author would like to thank Miss. M.L.Kendall for her encouragement and for pointing out some of the errors in the typed manuscript.

REFERENCES

1. Forrester, A. T., Gudmundsen, R. A. Johnson, P. O.
J.Opt.Soc.Am. 46, 339,(1956)

2. Jacobsen, E., Harrison, G. R.
J.Opt.Soc.Am. 39, 1054,(1949)

3. Meggers, W. F., Westfall, F. O.,
J.Res.Natl.Bur.Std. 44, 447, (1950)

4. Aschenbrand, et. al.
J.Opt.Soc.Am.42, 818,(1952)

5. Corliss et. al.
J.Opt.Soc.Am. 43, 398, (1953)

6. Tomkins, F. S., Fred. M.
J.Opt.Soc.Am. 47, 1087,(1957)

7. Fastie, W. C.
J.Opt.Soc.Am. 42, 641, (1952)

8. Fastie, W. C.
J.Opt.Soc.Am. 42, 647, (1952)

9. Rao, K. N., Humphreys, C. J., Rank, D. H.
Wavelength Standards in the Infrared,A
Academic Press (Inc.), 1966

10. Rao, K. N., Fraley, P. E.
Appl.Opt. 2, 1127, (1963)

11. Rank, D. H., Eastman, D. P. Rao, B. S. and Wiggins, T. A.,
J.Opt.Soc.Am. 51, 929, (1961)

12. Rank, D. H., et. al.
J.Opt.Soc.Am. 50, 657, (1960)

13. Handbook of Chemistry and Physics,
Ed.46, Pg.B148-B241, (1965-1966)

14. Pinnington, E. H.,
Ph.D. Thesis,(1962)

15. M.I.T. Wavelength Tables
by A. Harrison,
Wiley, New York

16. Corliss, C. H., Meggers, W. F.,
J.Res.Natl.Bur.Std. 61, 269, (1958)

17. Rupert, C. S.,
J.Opt.Soc.Am. 42, 779, (1952)

18. Fisher, R. A.,
J.Opt.Soc.Am. 49, 1100, (1959)

19. Douglass, A. E., and Sharma, D.,
J.Chem.Phys. 21, 448, (1953)

20. Bovey, L.,
Research 13, 363, (1960)

21. Worden, E. F., Gutmacher, R. G. and Conway, J. G.,
Appl.Optics 2, 707, (1963)

22. Robinson, D. and Lenn, P. D.,
Appl.Optics 6, 983, (1967)

23. Harrison, G.R., Lord, F.C., and Loofbourow, J.R.
Practical Spectroscopy,
Blackie and Sons Ltd., LON.

24. Peck, E. R.,
J.Opt.Soc.Am. 45, 795, 931, (1955)

25. Sullivan, S. A.,
J.Opt.Soc.Am. 43, 1031, (1955)

26. Rao, K. N., Humphreys, C. J. and Rank, D. H.,
Wavelength Standards in the Infrared,
Academic Press, N.Y.

27. Meggers, W. F., Corliss, C. H., and Scribner, B. F.,
Tables of Spectral Line Intensities
Natl. Bur. Std. Monograph 32, (1961)

28. Errors of Observation and their treatment
by J. Topping

29. Steers, E. B. M.,
Spectrochim.Acta 23B, 135, (1967)

30. Towers, T. D.,
Elements of Transistor Pulse Circuits
D. van Nostrand Co.

31. Rogers, G. Private Communication

32. Moore, C. E., N.B.S. Atomic Energy Levels
Vol. III, pp.145, (1958)

33. Tables of Wavenumbers Vol. I and II, NBS Monograph 3, (1960)
Coleman, C., Bozman, W. R., Meggers, W. F.

34. Harrison, G. R., Rev.Sci.Instr. 4, 581, (1933)

35. Marquet, L. C. and Davis, S. P.,
J.Opt.Soc.Am. 55, 471, (1965)

36. The Theory of Atomic Spectra,
E. U. Condon and G. H. Shortley, U.P., (1964)

37. White and Eliason, Phys. Rev. 44, 753, (1933)

38. Kessler, K. C., Prusch, S. B. and Stegun, I. A., J.Opt.Soc.Am. 46, 1043, (1956)

39. Spector, N., J.Opt.Soc.Am. 56, 341, (1966)

40. Steins, J., J.Opt.Soc.Am. 57, 355, (1967)

41. Bovey, L., Research 13, 363, (1960)

42. Steers, E. B. M., Private Communication

43. Slater, J.
Quantum Theory of Atomic Structure, Vol. I, II.
McGraw-Hill Book Company, Inc. N.Y.

44. Cowan, R. D.,
J.Opt.Soc.Am. 58, 808, (1968)

45. Trees, R. E., Cahill, W. F. and Rabinowitz, P.,
J.Res.Natl.Bur.Std. 55, 335, (1955)

46. Racah, G.,
Bul.Res.Council Israel 8F,1, (1959)

47. Racah, G.,
Phys.Rev. 61, 186, (1942)
Phys.Rev. 62, 438, (1942)
Phys. Rev.62, 367, (1943)

48. Kuhn, H. G.,
Atomic Spectra
Longmans, Green and Co. Ltd.

49. Gehatia, M.,
Phys.Rev. 94, 618, (1954)

50. Trees, R. E.,
Phys.Rev. 83, 756, (1951)

51. Wybourne, B. G.,
Spectroscopic Properties of Rare Earths,
John Wiley and Sons, Inc., N.Y.

52. Brink, D. M. and Satchler, G. R.,
Angular Momentum,
Clarendon Press, Oxford

53. Biedenharn, L. C., Blatt, J. M. and Rose, M. E.,
Rev.Mod.Phys. 24, 249, (1952)

54. Wilkinson,
The Algebra of Eiganvalue Problems

55. Ralston, A. and Wilf, H. S.,
Mathematical Methods for Digital Computers,
John Wiley and Sons, Inc.,N.Y.

56. Coster, D. and van Heresy,
Nature 111, 79, (1923)

57. Spector, N.,
J.Opt.Soc.Am. 57, 308, (1967)

58. Spector, N.,
J.Opt.Soc.Am. 57, 312, (1967)

59. Trees, R. E.,
Phys.Rev. 83, 756, (1951)

60. Racah, G.,
Phys.Rev. 85, 381, (1952)